UNIVERSITÀ DI PARMA

UNIVERSITA' DEGLI STUDI DI PARMA

DOTTORATO DI RICERCA IN
"*MEDICINA MOLECOLARE*"

CICLO XXXIV

Dottorato di ricerca a tema vincolato:

"Biostimolazione laser nella riparazione tissutale"

"Photobiomodulation in tissue repair"

Coordinatore:
Chiar.mo Prof. Prisco Mirandola

Tutore:
Chiar.mo Prof. Paolo Vescovi
Co-Tutore:
Chiar.mo Prof. Roberto Sala

Dottoranda: Dott.ssa Giulia Ghidini

Anni Accademici 2018/2019 – 2020/2021

Summary

INTRODUCTION

LASER AND PHOTOBIOMODULATION

The LASER (acronym of "Light Amplification by Stimulated Emission of Radiation", or in Italian "amplification of light by stimulated emission of radiation") is an optoelectronic device capable of emitting a coherent beam of light, that is by definition unidirectional, monochromatic and in phase.

These instruments are classified according to the IEC 60825 standards according to the danger to human health and their use in dentistry is well integrated into daily clinical practice.

Each active medium, properly excited once connected to alternating current, will emit a peculiar wavelength that will have the ability to interact with matter in a specific way.

Chromophores are the molecules responsible for the absorption of optical radiation and the coloring of the tissue.

The absorption curves of the main chromophores present in human tissues depends on the type of LASER i.e. the wavelenght emitted.

By dosing the amount of energy and the timeframe of its delivery to irradiated tissues, the clinician can exploit 4 different effects of laser light: 1) photochemical, 2) photomechanical, 3) photothermal and 4) photoablative.

The term "Photobiomodulation" (PBM) refers to the intra-cellular action of modulation of biological processes in irradiated tissues. This branch of laser application has been called over time that different terms, such as: biostimulation, photostimulation, Low Level Laser Therapy (LLLT), Low Intesity Laser Therapy (LILT), all however refer to the same non-invasive biomodulating therapy [1].

In vitro and clinical studies have demonstrated four main actions of laser photobiomodulation:

1) analgesic effect;

2) anti-edema effect;

3) decontaminating effect;

4) effect of inhibition or activation of intra-cellular processes.

Photobiomodulation is a characteristic of lasers with a wavelength between 600 nm and 1064 nm, this range is called "therapeutic window".

In international literature, all wavelengths with biostimulation or biomodulation activities in the oro-maxillofacial area are reported [2].

To achieve PBM, very low energy are delivered for long application's times.

The mechanism of action underlying LLLT is probably of photochemical nature and yet to be completely understood.

The primary photoaceptors may be found in the mitochondrial respiratory chain or at the level of the cell membrane. Cellular photoreceptors are considered to

be cytochromophores such as endogenous porphyrins and molecules of the respiratory chain such as cytochrome c-oxidase.

The absorption of laser light by the components of the respiratory chain causes a short-term activation of the respiratory chain itself and the oxidation of the NADH, causing changes in the redox state of the mitochondria and cytoplasm. The activation of the electron transport chain determines an increase in the membrane potential of the mitochondria and an increase in the production of ATP, these cause the alkalinization of the cytoplasm and, as a final consequence, the triggering of the synthesis of nucleic acids and the acceleration of cell metabolism[3].

It has been hypothesized that the action of the LLLT may also take place through the induction of the formation of "singlet oxygen", a form characterized by high energy and high reactivity. The LLLT determines an increase in the amount of mRNA at the base of the synthesis of type I and type III collagen and therefore a stimulating action on the production and repair of mucousa and bone tissue.

LLLT may also stimulates cell proliferation by inducing cell cycle regulatory proteins and cell differentiation.

No studies, to date, have clearly stated a pathway in which laser light involvement is clearly explained, so PBM still remains an interesting subject of study since biological effects have been widely observed in all medical branches, not only dental, but not fully explained [4].

LITERATURE REVIEW

As first step for the present thesis work we aimed to overview the state of the art regarding photobiomodulation and its application on stem cells.

Mesenchymal derived stem cells have emerged as a popular and versatile tool in the field of regenerative medicine and a growing interest as been shown for their use in tissue's engineering during the last decades.

Photobiomodulation has been investigated in *in vitro* and in *in vivo* experiments in association with mesenchymal derived stem cells; most common studied stem cells derive from bone marrow (BMSC), from adipose tissue (ADSC) or dental tissues (either from dental pulp or periodontal ligament).

Photobiomodulation is the newest and most common noun recently introduced to identify the application of low doses of laser light for long periods of time.

The variety of terms previously used to identify this medical laser application includes: cold laser therapy, soft laser therapy, low level light therapy, low level laser therapy, biostimulation and photobiostimulation.

However, the term "stimulation" implies a raising of levels in physiological or nervous activity of the body or any biological system but, as shown by many published studies, the laser light absorbed by tissues is capable to induce down-regulation of specific intracellular pathways, not only up-regulation of cell's metabolism.

Therefore, the noun “photobiomodulation” appears to best describes the totality of the effects performed by laser light applications.

First, the electronic search was conducted with PubMed database for English-language articles published until May 2019.

Following 15 MeSH terms and keywords were used separately and/or in combination: Photobiomodulation, Low Level Laser Therapy; Low Level Light Therapy; Low Level Laser Irradiation; Low Level Light Irradiation; LLLT; LLLI; Stem Cells; Bone Marrow; Adipose; Periodontal Ligament; Dental Pulp; Mesenchymal Stem Cell; Cell Proliferation; Cell Differentiation.

The selection of studies was initiated by the review of articles’ titles: eligible papers were characterized as *in vitro* experimental studies evaluating the use of photobiomodulation on bone marrow (BMSC), adipose (ADSC) or dental (DMSC) stem cells in order to promote their proliferation and/or differentiation.

Selected articles had their abstracts analyzed: articles without a case - control design were excluded.

Full text of 92 articles were read and 59 excluded due to lack of data and details regarding the experiment setup, the possibility to compare and replicate experiment was considered key during the inclusion/exclusion process of this review.

Finally, 25 studies were included in this literature review, as shown in Figure 1; studies were grouped by origin of harvested cells.

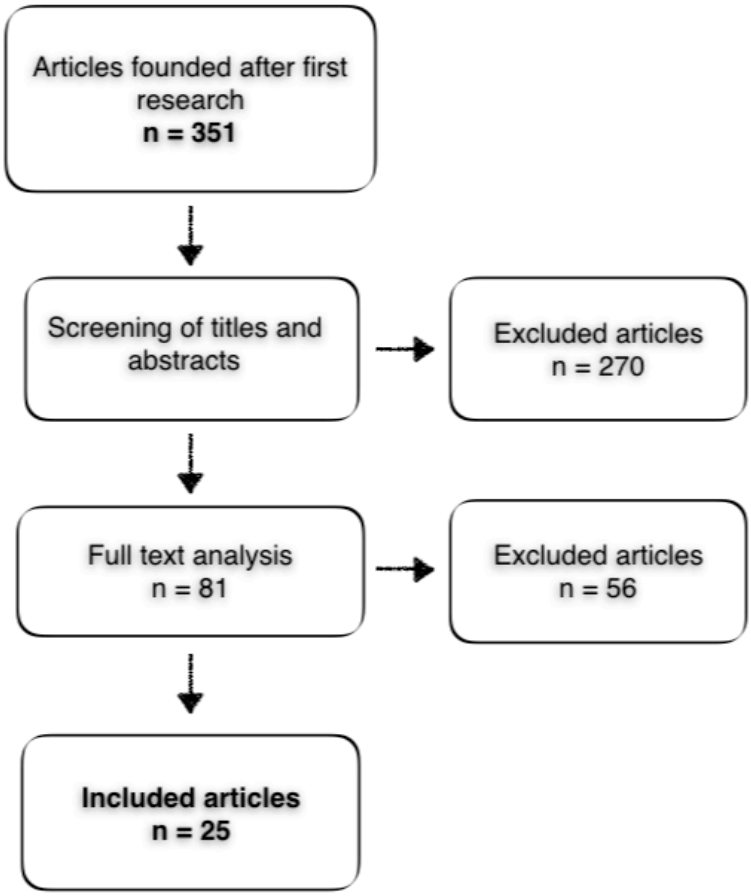

Figure 1: Flowchart of article's selection process.

For every included study, Fluence values, laser wavelength and type of laser, Power Output and Power Density settings and time with schedule of application were analysed.

Main focus was on proliferation and / or differentiation rates: we highlighted assays performed to evaluate this two biological process.

Twenty-five papers that met the search criteria and were included in this review starting from 351 references obtained are shown in the following table (Table 1).

Table 1: Index of 25 articles included in the literature review.

Author(s) - Year of pubbl.	Title
Abramovitch-Gottlib et al.- 2005 [5]	"Low level laser irradiation stimu- lates osteogenic phenotype of mes- enchymal stem cells seeded on a three-dimensional biomatrix"
Barboza et al. - 2013 [6]	"Low-level laser irradiation induces in vitro proliferation of mesenchymal stem cells"
Bouvet-Gerbettaz et al. - 2009 [7]	"Effects of Low-Level Laser Therapy on Proliferation and Differentiation of Murine Bone Marrow Cells Into Osteoblasts and Osteoclasts"
Choi et al. - 2013 [8]	"Low-level laser therapy promotes the osteogenic potential of adipose- derived mesenchymal stem cells seeded on an acellular dermal ma- trix"
Eduardo et al. - 2008 [9]	"Stem Cell Proliferation Under Low Intensity Laser Irradiation: A Preliminary Study"
Fekrazad et al. - 2015 [10]	"The effects of combined low level laser therapy and mesenchymal stem cells on bone regeneration in rabbit calvarial defects"
Fernandes et al. - 2015 [11]	"Effects of low-level laser therapy on stem cells from human exfoliated deciduous teeth"
Giannelli et al. - 2012 [12]	"Photoactivation of Bone Marrow Mesenchymal Stromal Cells With Diode Laser: Effects and Mechanisms of Action"
Hendudari et al. - 2016 [13]	"Combined effects of low-level laser therapy and human bone marrow mesenchymal stem cell conditioned medium on viability of human dermal fibroblasts cultured in a high-glucose medium"
Hou et al. -2008 [14]	"In Vitro Effects of Low-Level Laser

	Irradiation for Bone Marrow Mesenchymal Stem Cells: Proliferation, Growth Factors Secretion and Myo- genic Differentiation"
Merigo et al. - 2016 [15]	"Green laser light irradiation enhances differentiation and matrix mineralization of osteogenic cells"
Min et al. - 2015 [16]	"Effect of Low-Level Laser Therapy on Human Adipose-Derived Stem Cells: In Vitro and In Vivo Studies"
Moura-Netto et al. - 2016 [17]	"Low-intensity laser phototherapy enhances the proliferation of dental pulp stem cells under nutritional deficiency"
Mvula et al. - 2010 [18]	"Effect of low-level laser irradiation and epidermal growth factor on adult human adipose-derived stem cells"
Nagata et al. - 2013 [19]	"Bone marrow aspirate combined with low-level laser therapy: A new therapeutic approach to enhance bone healing"
Park et al. - 2015 [20]	"Adipose-derived stromal cell cluster with light therapy enhance angiogenesis and skin wound healing in mice"
Pereira et al. - 2012 [21]	"Laser irradiation did not increase the proliferation or the differentiation of stem cells from normal and inflamed dental pulp"
Santos de Oliveira et al. - 2015 [22]	"Effects of low level laser therapy on attachment, proliferation, and gene expression of VEGF and VEGF receptor 2 of adipocyte-derived mesenchymal stem cells cultivated under nutritional deficiency"
Soares et al. - 2015 [23]	"Effects of laser therapy on the proliferation of human periodontal ligament stem cells"

Soleimani et al. - 2012 [24]	"The effects of low-level laser irradiation on differentiation and proliferation of human bone marrow mesenchymal stem cells into neurons and osteoblasts—an in vitro study"
Theocharidou et al. - 2017 [25]	"Odontogenic differentiation and biomineralization potential of dental pulp stem cells inside Mg-based bioceramic scaffolds under low-level laser treatment"
Tuby et al. - 2011 [26]	"Induction of Autologous Mesenchymal Stem Cells in the Bone Marrow by Low-Level Laser Therapy Has Profound Beneficial Effects on the Infarcted Rat Heart"
Wang et al. - 2012 [27]	MicroRNA-193 Pro-Proliferation Effects for Bone Mesenchymal Stem Cells After Low-Level Laser Irradiation Treatment Through Inhibitor of Growth Family, Member 5"
Wu et al. - 2013 [28]	"Low-Power Laser Irradiation Suppresses Inflammatory Response of Human Adipose-Derived Stem Cells by Modulating Intracellular Cyclic AMP Level and NF-kB Activity"
Zaccara et al. - 2015 [29]	"Effect of low-level laser irradiation on proliferation and viability of human dental pulp stem cells"

The literature review showed that photobiomodulation positively influences proliferation and differentiation of stem cells in almost the totality of included *in vitro* studies.

A lack of uniformity of parameters and evaluation systems was highlighted: grate varieties of wavelengths and laser settings (such as power density, power

output, time of irradiation) were used. Each experimental setting included different assays and markers for assessing cell viability and sample size.

No univocal comparison between studies was possible.

However, it was possible to identify the most frequently used wavelength: in most studies photobiomodulation was performed with a visible red-wavelength, mainly of 660 nm (57,14%).

Fluence values between 0.5 and 5 J/cm2 were most frequently chosen as setting (75,92%), even if it must be taken into consideration that the resulting value of Fluence follows a variety of different setting such as power density, power output, time of irradiation.

Conclusions of this review highlighted the main problem in the current state of the art: the impossibility of comparing different studies with each other due to the lack of uniformity of protocols and no univocal indications for user to set laser's parameters during photobiomodulation.

EX VIVO STUDY

In order to ground and design a case-control *in vitro* study this preliminary *ex vivo* study aimed to assess the possible interaction between complex systems and laser light through irradiation of different soft tissue's samples. Main focus was on measuring how deep the light beam was able to reach cells' layers. Samples of soft and hard tissues absorption of a 645 nm diode laser was tested

to verify if and eventually how deep the laser light was able to reach inside the irradiated tissue.

A 645 nm wavelength diode laser was selected red wavelength was chosen in order to allow further comparison with the most used wavelength in published articles found in literature.

Due to known similarities to human tissues, mandible were harvested from a swine mandible preserved in 500 Samples were collected 24 h before the experiment was conducted. Chosen power output value was set as 220 mW, measurements were performed with a power-meter located underneath the irradiated tissue.

A laser tip with measured 0.337 cm2 of area was choosen for irradiation (Figure 2).

Figure 2: Laser tip.

Emission was performed perpendicularly to the power meter at a circa 2 cm of distance: an actual power output of 168 mW was detected (Figure 3).

Irradiation was performed for 113 seconds, no support system was used.

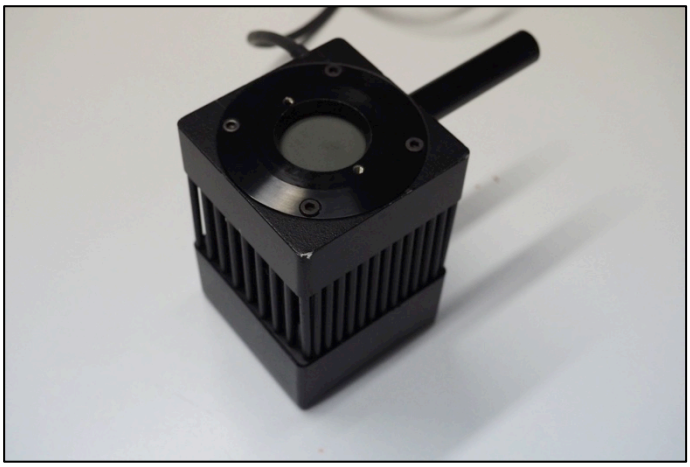

Figure 3: Power meter.

Before tissue irradiation, measurements were performed with and without plastic protection devices around the laser tip and the power meter, to simulate daily practitioner's work setting, as shown in Figure 4.

Figure 4: Preliminary measurements without plastic protection devices.

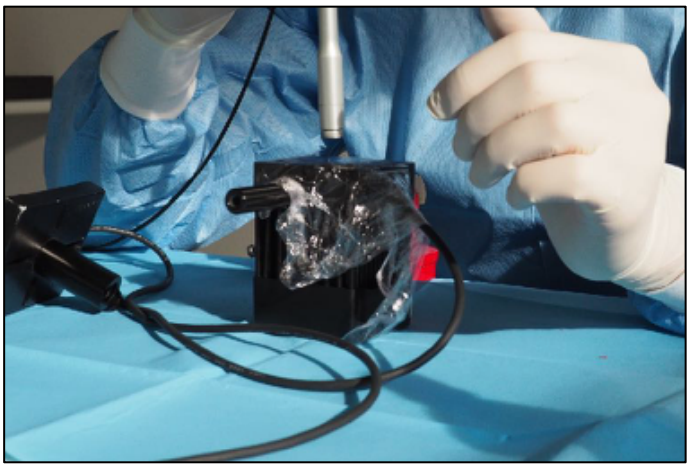

Figure 4: Preliminary measurements with plastic protection devices.

A sample of periosteum of 0.45 mm of thickness, two mucosae samples measuring 0.5 mm and 1 mm, three samples including both mucosae and periosteum of 1 mm, 1.3 mm ad 1.65 mm of thickness were harvested for the analysis of soft tissues (some of the soft tissue samples are displayed in Figure 5).

Figure 5: Example of soft tissue samples.

Two samples of cortical bone measuring 4.4 mm and 4.7 mm of thickness and 2 samples of spongeous bone measuring 2.45 mm and 2.9 mm were harvested for the analysis of hard tissues (some of the hard tissue samples are displayed in Figure 6).

Figure 6: Example of hard tissue samples.

After 10 cycles of irradiation, data-log were converted into graphics: on axis x is time in seconds (s) and on axis y is power output in milliwatt (mW) (Figure 7).

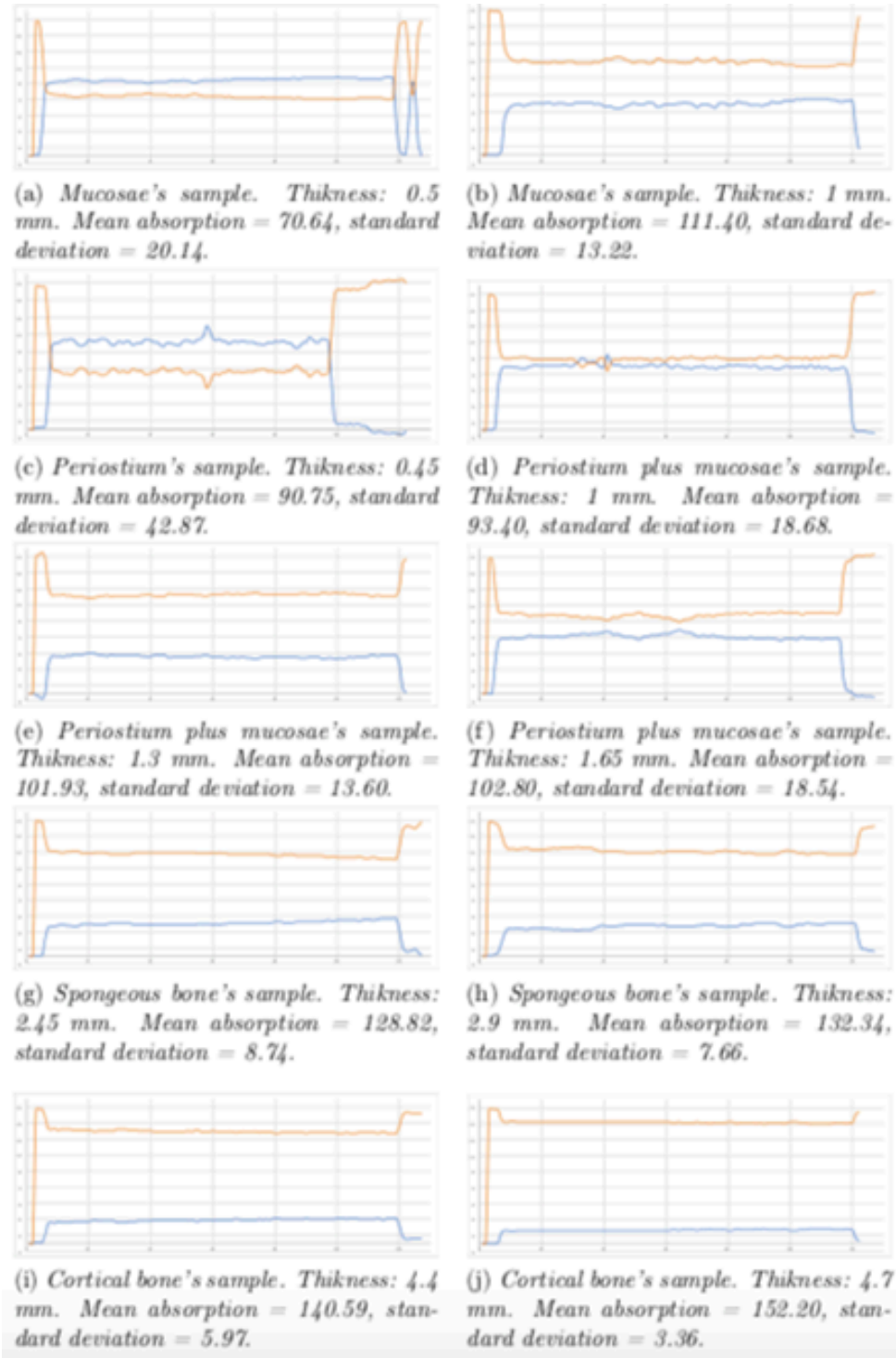

(a) *Mucosae's sample. Thikness: 0.5 mm. Mean absorption = 70.64, standard deviation = 20.14.*

(b) *Mucosae's sample. Thikness: 1 mm. Mean absorption = 111.40, standard deviation = 13.22.*

(c) *Periostium's sample. Thikness: 0.45 mm. Mean absorption = 90.75, standard deviation = 42.87.*

(d) *Periostium plus mucosae's sample. Thikness: 1 mm. Mean absorption = 93.40, standard deviation = 18.68.*

(e) *Periostium plus mucosae's sample. Thikness: 1.3 mm. Mean absorption = 101.93, standard deviation = 13.60.*

(f) *Periostium plus mucosae's sample. Thikness: 1.65 mm. Mean absorption = 102.80, standard deviation = 18.54.*

(g) *Spongeous bone's sample. Thikness: 2.45 mm. Mean absorption = 128.82, standard deviation = 8.74.*

(h) *Spongeous bone's sample. Thikness: 2.9 mm. Mean absorption = 132.34, standard deviation = 7.66.*

(i) *Cortical bone's sample. Thikness: 4.4 mm. Mean absorption = 140.59, standard deviation = 5.97.*

(j) *Cortical bone's sample. Thikness: 4.7 mm. Mean absorption = 152.20, standard deviation = 3.36.*

Figure 7: Graphics of irradiated soft and hard tissue smples. On axis x is time in seconds (s) and on axis y is power output in milliwatt (mW). Orange line = absorption, blue line = transmission.

For each sample values of mean absorption and standard deviation were calculated.

Calculated values of mean absorption showed how higher thicknesses coincide with lower transmissions. No differences were highlighted between detected measurements when laser was used with or without plastic protection devices.

We attempted to answer to the main question of this *ex vivo* study (how deep does laser light effectively reach cells in the irradiated tissue?) by the analysis of the outcomes.

As shown in graphics: if two lines are present, one portion of laser wavelength is absorbed while the other is transmitted. In every analyzed sample laser light was never completely absorbed nor completely transmitted by cell layers. It is important to consider not only the transmission of light inside irradiated tissues, but also cells not directly reached by laser- light can be stimulated anyway by other phenomena such as scattering and diffusion. Furthermore, once a single cell has been biostimulated and its metabolism changes, connections between other cells in same tissues dictate pathways activation and the variation of the whole biological system.

Thicker tissues samples showed higher values of absorption, while thinner tissues samples showed higher values of transmission. Cortical bone samples

seemed to absorb higher values of laser light, while spongeous bone seemed to transmit more. Calculated values of mean absorption showed how higher thicknesses coincide with lower transmissions for both the two types of investigated bone samples.

Likewise, calculated values of mean absorption in soft tissues samples showed how higher thicknesses coincide with lower transmissions.

It can be observed that the lack of a support of measurements and those areas of the graphics should not be taken into consideration.

Manual support of laser tip involves possible micro-movement of operator's hand, that can lead to variations of the emission angle, resulting in loss of coherence of the laser beam and scattering. It is important for the operator to remind that during and target tissues needs to remain as constant as possible, to deliver the same amount of energy to every irradiated area.

Finally, a finding of the present study is that sterile and non-sterile devices can be used to isolate to use non-disposable laser tips, avoiding further thus reducing energy dispersion.

After analysing results and comparing graphics, it can be concluded that red-light laser with 645nm wavelength can reach cells in each layer of measured bone tissues samples, both for cortical *ex vivo* experiment, conducted on swine mandible tissues established with the use of a power meter so that every tissue layer was reach by the laser beam. Since thickness of sample

tissues are comparable to human tissues, we can conclude that protocols using these laser features can reach every cell layer in target tissues; this could possibly lead to interactions or rather photobiomodulation of human cells.

PART I - IN VITRO STUDY ON SAOS-2

As said in the introduction of these thesis work, Photobiomodulation has garnered increasing attention thanks to a large number of controlled clinical trials that have proven its efficacy in various oral pathologies [30].

Nevertheless, the mechanism of action (MOA) is still a matter of debate and several hypotheses have been proposed. The one that has gained the most consensus regards the activation of cytochrome–c oxidase which acts as a mitochondrial photo-acceptor when irradiated by a He-Ne laser (633 nm) [31]. Upon cytochrome activation, more ATP is produced by mitochondria, signals generated by mitochondria can target the nucleus and regulate gene expression[32]. Red and infrared light increase cAMP production, which, in turn, activates protein kinase A (PKA)[33], [34] and modulates reactive oxygen species (ROS) and Ca^{2+} concentrations. Thus, a signaling cascade begins, which promotes proliferation and cell differentiation, as well [31], [32].

When it comes to photobiomodulation, another tricky point is illustrated with the Arndt-Schulz law**:** Low doses have no effect - the biological effect appears only after increasing the energy, but the cells and tissues are damaged with greater energy. This issue was analyzed in a recent review by Huang[35]. It highlights that the amount of energy that reaches the cells is the principal factor in photobiomodulation therapy. In fact, many studies have analyzed the optical

proprieties of human tissues [36]–[38] with the aim of helping to design harmless protocols that promote tissue healing.

We noticed that all the experimental *in vitro* settings that we were able to retrieve with a pub-med search were developed with cells cultured in the presence of fetal bovine serum (FBS). The concentrations of FBS used were able, per se, to induce cell proliferation over time. Due to the fact that bleeding and clot formations are the first reactions following a traumatic injury, it is typical to employ high FBS concentration in an *in vitro* experimental setting. Since FBS induces cell growth, in order to correctly evaluate the efficacy of photobiomodulation, we designed a protocol in the absence of FBS growth factors.

The source of the growth factors we used is platelet-rich plasma. PRP was chosen because platelet growth factors are the first promoters of wound healing and it appears immediately after tissue injury, therefore, it is widely used in clinical practice [39]–[41].

MATERIALS AND METHODS

Cells culture and seeding

Saos-2 cells (catalog code: BS TLC 90 - IZSLER - Brescia, Italy), a human osteosarcoma cell line [42], were cultured in low glucose Dulbecco's Modified Eagle Medium (LG-DMEM) with 2 mM of glutamine and 10% FBS in a humidified atmosphere of 5% CO_2 in air at 37° C.

The medium was replaced every third day with a fresh one. For the experiments, cells were seeded into black 96-well plates (CorningCostar- Biosigma S.r.l.-Cona (VR) -Italy).

To avoid light scattering to adjacent cells, we seeded Saos-2 cells in alternate rows and columns so that each well with cells was surrounded by wells without cells and filled with PBS.

In order to imitate the complexity of the circumstances that develop in wounded tissue medicated with PRP to the greatest possible extent, the day after seeding, we layered PRP, containing $2691x10^3$ platelets/ml, on top of cells, and then we added 50µl of the medium.

To avoid thermal shock, we lodged the cell trays in special, customized aluminum plates during the irradiation time (Fig. 8a and b).

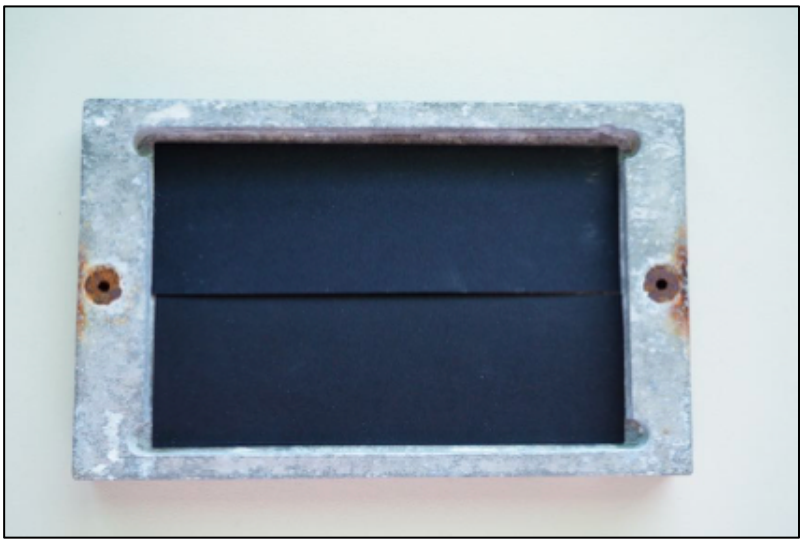

Figure 8a: Setting for temperature maintenance. Metallic cast with obscured background to avoid light scattering.

Figure 8b: Setting for temperature maintenance. 96-well plate positioned inside the customized metallic cast.

Cells were seeded at the density of $1x10^3$cells/well for the evaluation of proliferation rate and at the density of $5x10^3$ cells/well for the evaluation of differentiation.

PRP and medium characteristics

PRP was prepared by centrifugation and immediately frozen. 15 µl of calcium gluconate, 100 mg/ml solution, and 200 µl of defibrinated allogenic plasma were added to every 1 ml of defrosted PRP. Before jellification, 50 µl of this suspension was quickly dispensed into each well to cover the cells.

To evaluate the proliferation rate, the medium was prepared by adding 0.1% FBS, glutamine 2mM to LG-DMEM with phenol red.

For osteogenic differentiation assessment, the medium was composed as follows: LG- DMEM with phenol red, 0.1% FBS, glycerophosphate 2 mM, ascorbate 100 µM, proline 4 µg/mL, glutamine 2mM.

Radiation protocols, laser settings, and data collection

Photobiomodulation was performed at 645 (±10nm) wavelength with Raffaello laser diode (Dental Medical Technologies, DMT srl. Lissone, MB, Italy), protocols were applied every other day for a total of six applications.

Since no univocal setting, neither univocal fluence value nor the time of irradiation, was highlighted in the literature review as being the most efficient, we identified nine photobiomodulation protocols to investigate in order to compare the largest possible spectrum of variables. Since phenol red could interact with the laser beam, we previously tested the amount of energy effectively delivered to the cells with a power meter positioned below the plate with the wells filled with the medium used during the experiments. The instrument was properly set, taking into account this interference, to deliver the amount of energy reported in Table 1.

Three different energy density (or fluence) values (2 J/cm^2, 5 J/cm^2, and 10 J/cm^2) and three different times of irradiation (1 minute, 2 minutes, and 4 minutes) were combined as follows:

I. 2 J/cm^2 delivered in 1 minute;

II. 2 J/cm^2 delivered in 2 minutes;

III. 2 J/cm^2 delivered in 4 minutes;

IV. 5 J/cm^2 delivered in 1 minute;

V. 5 J/cm^2 delivered in 2 minutes;

VI. 5 J/cm^2 delivered in 4 minutes;

VII. 10 J/cm^2 delivered in 1 minute;

VIII. 10 J/cm^2 delivered in 2 minutes;

IX. 10 J/cm^2 delivered in 4 minutes.

We applied photobiomodulation every other day for a total of six times, and each experiment was replicated three times. Wells and corresponding irradiation protocols are shown in Figure 9a and b.

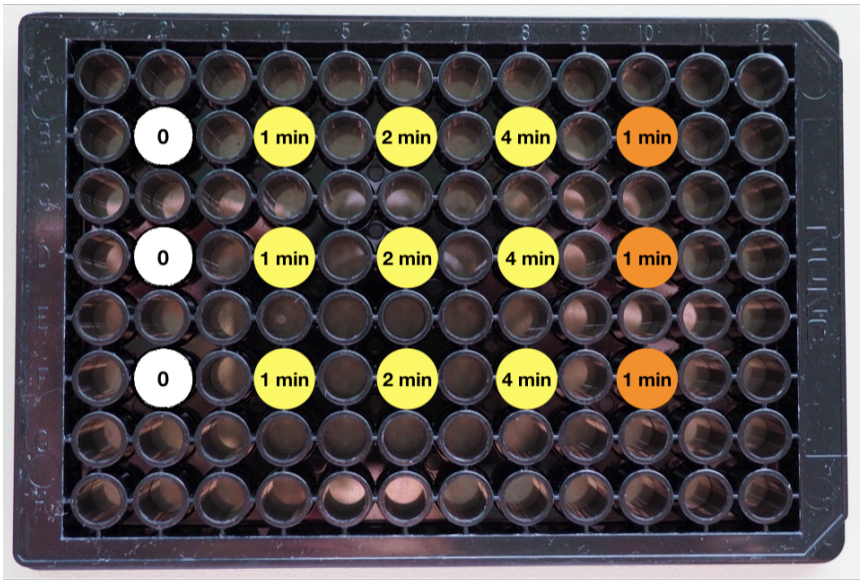

Figure 9a: Radiation setting. Wells and corresponding irradiation protocols are shown in the following way: white = no irradiation, yellow = 2 J/cm^2, orange = 5 J/cm^2, and red = 10 J/cm^2.

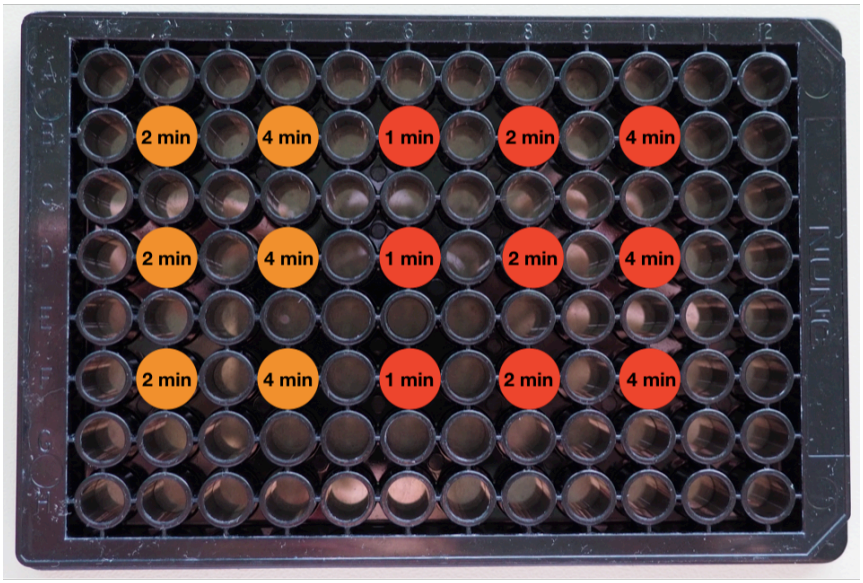

Figure 9b: Radiation setting. Wells and corresponding irradiation protocols are shown in the following way: white = no irradiation, yellow = 2 J/cm^2, orange = 5 J/cm^2, and red = 10 J/cm^2.

The area of the chosen laser tip measured 0.337 cm^2 and matches the area of a well in a 96 well plate.

Since there is a discrepancy between the Power Density reported on the laser monitor and the real power output at the tip of the laser, the manufacturer provided us with a conversion table with parameters to enter on the laser monitor in order to obtain the desired Fluence values for all nine protocols. Parameters are described in Table 2.

Table 2: Desired parameters *vs* parameters displayed on the laser's monitor.

Fluence delivered (J/cm^2)	Irradiation Time (min)	Fluence setting (J/cm^2)	Power Density setting (mW/cm^2)	Total Energy (J)	Power Output (mW)
2	1	6,7	110	3,3	55
2	2	9,6	80	4,8	40
2	4	14,4	60	7,2	30
5	1	11,4	190	5,7	95
5	2	15,6	130	7,8	65
5	4	21,6	90	10,8	45
10	1	21,9	360	10,8	180
10	2	22,8	190	11,4	95
10	4	31,3	130	15,6	65

We always irradiated the cells in a vertical laminar flow hood (Biohazard Aura - B4), fixing the laser tip to a metallic semi-articulated hand. Plates were

positioned on a fixed support parallel to the laser tip. We checked perpendicularity with a spirit level (Figure 10).

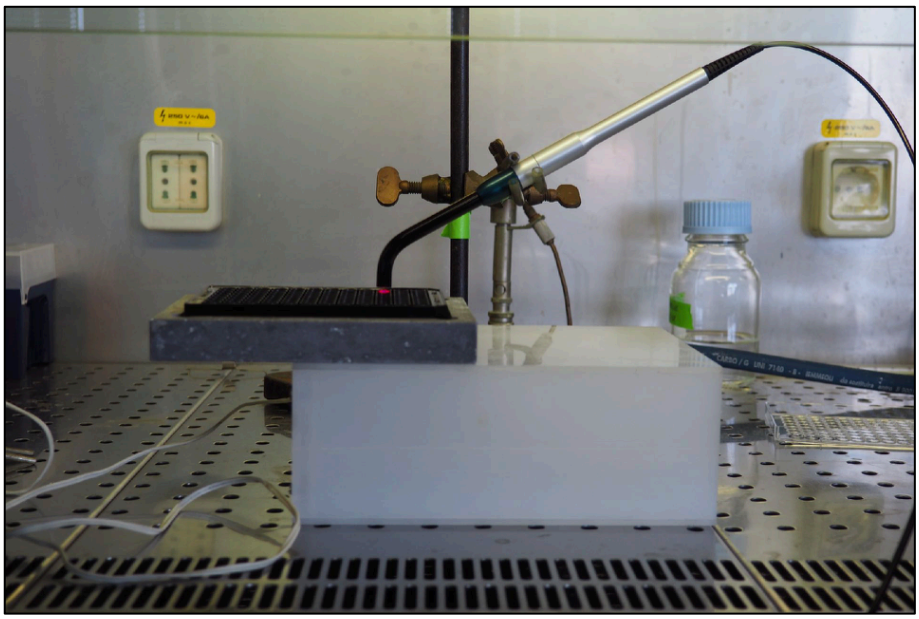

Figure 10: Laser settings inside the hood.

Cell viability was evaluated by resazurin assay [16] before every laser irradiation with the exception of the last day. After cell viability assay, cells were washed before irradiation with PBS and the medium was changed. 96-well plates were stored in the dark for one hour before using the fluorimeter.

We assessed cell differentiation by Alizarin-red Sigma - Aldrich (ARS) assay 48 hours after the last laser irradiation for the evaluation of calcium deposits in the cell culture.

Alizarin Red S staining

The staining of calcium salts with Alizarin Red was carried out accordingly to a previously published method.[17] Cells were washed with PBS and fixed with 4%

formaldehyde solution at RT. Next, 40 mM Alizarin Red S solution (pH 4.2) was added to each well. After 30 minutes, the cells were rinsed five times with ddH_2O. To measure Alizarin Red S concentration, 200 µL of 10% acetic acid were added to each well and incubated for 30 minutes at RT. The slurry was then transferred into a new tube. After vigorous shaking for 30 seconds, the samples were heated to 85°C for 10 minutes. Then, samples were chilled on ice for five miuntes and centrifuged at 20000 rpm for 15 minutes. An Alizarin Red S standard curve was prepared with serial dilutions of Alizarin Red ranging from 10 mM to 10 µM, and absorbance was measured at 405 nm with an Enspire microplate reader (Perkin Elmer, Waltham, Massachusetts, USA).

Statistical analysis

Data were expressed as Mean ± SD of three independent experiments. Growth curves were generated with GraphPad Prism 6.0 software and analyzed with Two-way ANOVA. Statistical significance was corrected for multiple comparisons using the Holm-Sidak method, and $p<0.05$ was considered the level of statistical significance. Mineralization was analyzed with a two-way ANOVA analysis, which was followed by a T-test, and the statistical significance was corrected for multiple comparisons using the Holm-Sidak method, and $p<0.05$ was considered the level of statistical significance. Data are expressed as mean value ± standard deviation of three independent experiments.

RESULTS

The effects of PRP on the viability of the Saos-2 cell line are shown in figure 4, whereas the consequences of the laser irradiation on cell population are outlined from figure 5 to figure 8. Measurements were performed before laser irradiation every other day.

When PRP was layered on top of Saos-2 cells, it induced a marked increase in cell proliferation that was statistically evident from the fifth day ($p<0.0001$).

In the presence of PRP, resazurin assay revealed a growth pattern of cells that were better fitted by Sigmoidal curves for up to 14 days of culture (Fig. 11): x-axis: time (days); y-axis: resorufin fluorescence values. Data are expressed as mean–SD of three independent experiments. Linear regression analysis was performed with GraphPad software. In the presence of 0.1% FBS, the cells did not grow. The addition of PRP induced cell proliferation after the lag phase. During the subsequent medium changes, the PRP was washed out and no further cell growth was observed.

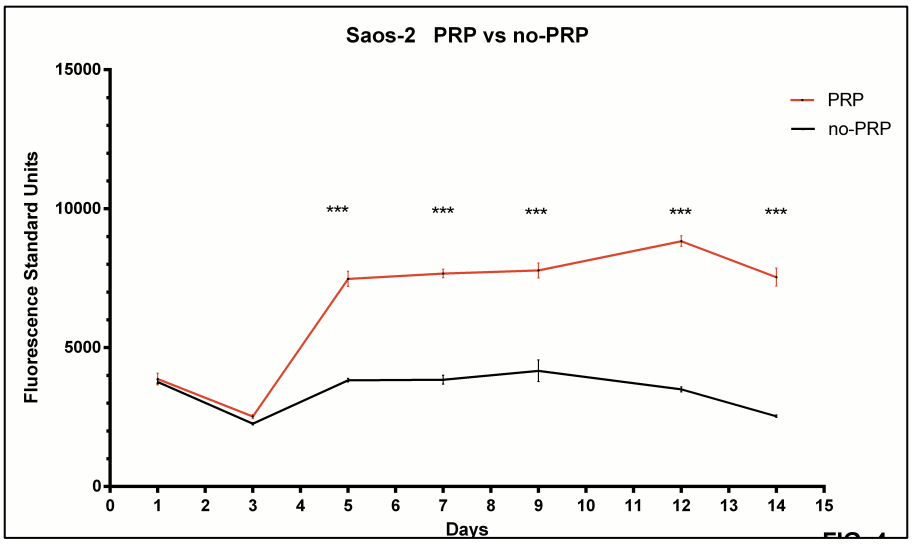

Figure 11: Monitoring of Saos-2 cell growth in the presence (red line) or absence (black line) of PRP with 0.1% FBS.

In the absence of PRP, but with 0,1% FBS, the overall slopes of the growth curves observed after laser stimulations were identical (F=0.0666544; DFn=9; DFd=190; p=0.9999), and data were best fitted with linear regression for up to 12 days of culture.

The Y intercepts were not significantly different (F=0.132277; DFn=9; DFd=199; p=0.9988); therefore, it was possible to calculate one Y intercept for all the data, meaning that without growth factors, the laser was not able to induce cell proliferation. At 14 days, an overall decrease in cell vitality was detected independently from the culture conditions. This effect was probably due to the lack of growth factors able to support further Saos-2 cell viability (Fig. 12).

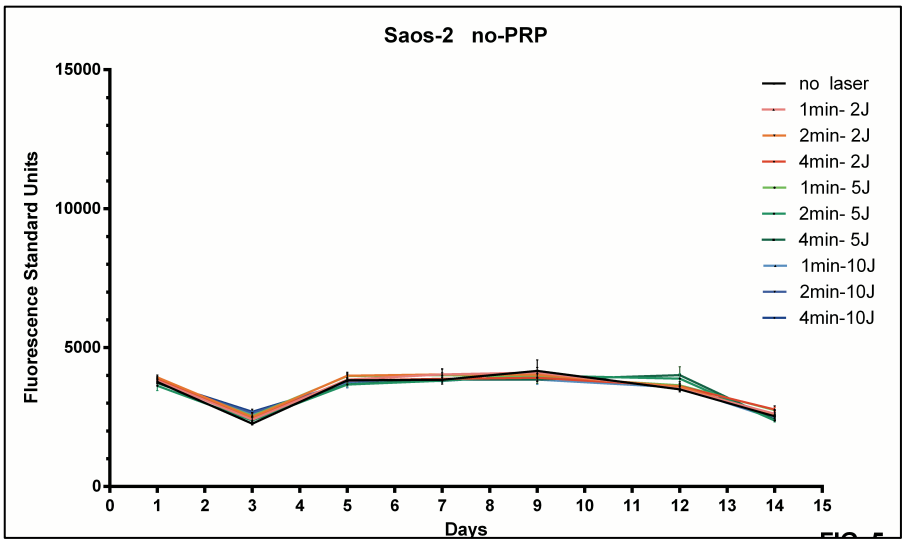

Figure 12: The effects of laser irradiati on the proliferation of the Saos- 2 cell line in the absence of PRP, but in the presence of 0.1% FBS. X-axis: time (days); y-axis: resorufin fluorescence values. Data are expressed as mean–SD of three independent experiments. In these conditions, no cell growth was detected.

In the presence of PRP, resazurin assay revealed a growth pattern of cells that were better fitted by Sigmoidal curves.

The comparison of the growth curves induced by laser fluence of 2 J/cm^2 (no laser: r^2=0.94; 2J-1min: r^2=0.9; 2J-2min: r^2=0.91; 2J-4min: r^2=0,93) did not detect significant differences (p=0.587). This analysis indicates a superimposable growth pattern of Saos-2 cells under all the tested conditions until the end of the experimental period (Fig. 13); data are expressed as mean–SD of three independent experiments. The comparison of curve fittings was analyzed with two-way ANOVA. Statistical significance was determined using the Holm-Sidak method. The biostimulation did not induce a further increase of cell growth. ANOVA, analysis of variance.

.

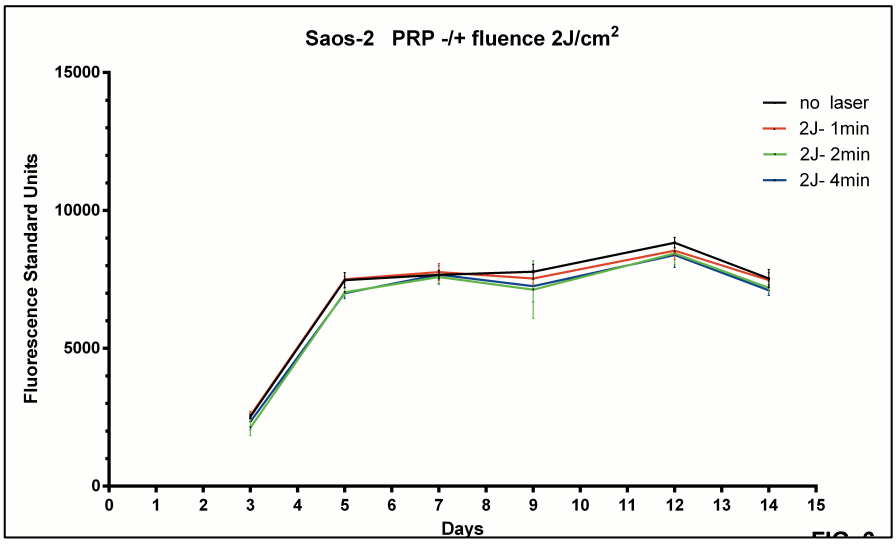

Figure 13: Saos-2 cell growth in the presence of PRP, with or without laser irradiation, with a fluence of 2J/cm^2. X-axis: time (days); y-axis: resorufin fluorescence values.

Furthermore, when the fluence of 5 J/cm^2 was delivered in 1 minute, there was no significant difference in cell growth; on the contrary, when 5 J/cm^2 was dispensed in 2 minutes or 4 minutes, the fitting curves differed significantly ($p<0.0002$) (Fig.14). Data are expressed as mean – SD of three independent experiments. The comparison of curve fittings was analyzed with two-way ANOVA. Statistical significance was determined using the Holm-Sidak method. When the fluence of 5 J/cm2 was delivered in 1 min, there was no significant difference in cell growth when compared to non-irradiated cells; on the contrary, when 5J/cm2 was dispensed in 2 or 4min, the growth curves showed significant differences ($p < 0.002$).

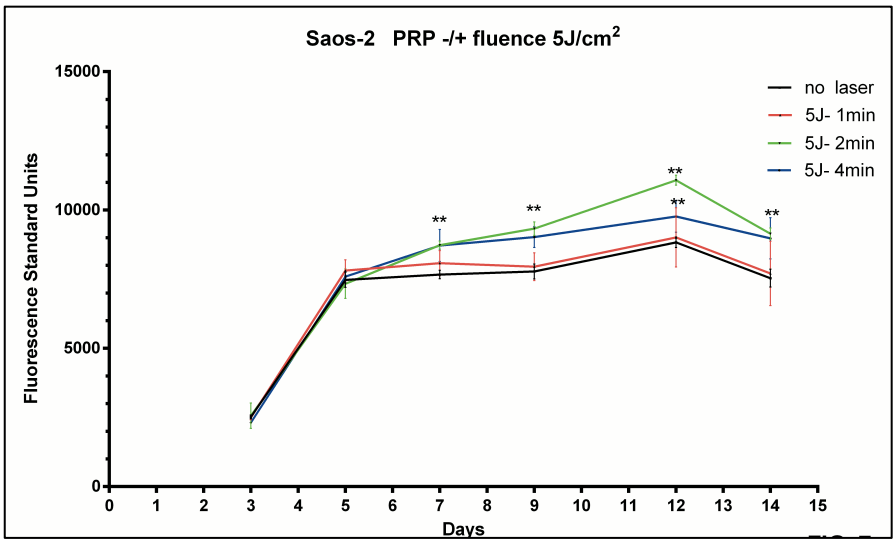

Figure 14: Saos-2 cell growth in the presence of PRP, with or without laser irradiation, with a fluence of 5J/cm2. X-axis: time (days), y-axis: resorufin fluorescence values.

When the protocol with a fluence of 10 J/cm^2 was applied, a statistically significant difference in cell growth was only evident when a total of 10 J/cm^2 was administered in 4 minutes.

($p<0.05$) (Fig. 15).

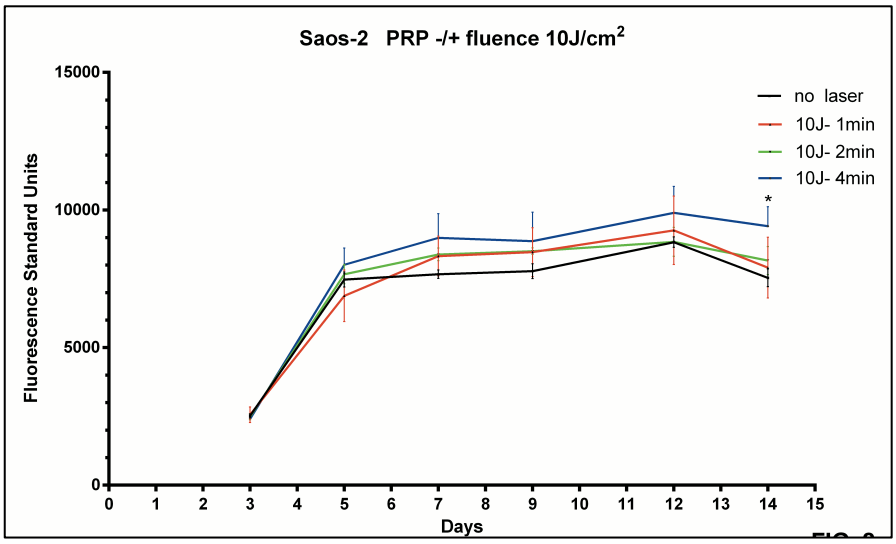

Figure 15: Saos-2 cell growth in the presence of PRP, with or without laser irradiation, with a fluence of 10 J/cm^2. X-axis: time (days), y-axis: resorufin fluorescence values.

Mineralization, as a marker of cell differentiation, was assessed by Alizarin-red assay. In the absence of PRP, we did not observe any difference in Alizarin red staining due to laser stimulation with different fluence values (Tab. 3).

Table 3: Mineralization od Saos-2 cell's measured as Alizarin Red concentration.

		Alizarin, mM (mean ± SD)		
Fluence	**Time**	**no PRP**	**PRP**	**P value**
0 J/cm²		0,079 ± 0,006	0,634 ± 0,095	0.004
2 J/cm²	1 min	0,068 ± 0,004	0,650 ± 0,118	0.007
	2 min	0,068 ± 0,003	0,637 ± 0,054	0.0008
	4 min	0,074 ± 0,006	0,523 ± 0,052	0.001
5 J/cm²	1 min	0,091 ± 0,008	0,712 ± 0,117	0.002
	2 min	0,071 ± 0,003	1,129 ± 0,127	0.0003
	4 min	0,073 ± 0,006	0,769 ± 0,081	0.0003
10 J/cm²	1 min	0,069 ± 0,007	0,847 ± 0,043	0.0002
	2 min	0,067 ± 0,008	0,753 ± 0,050	<0.0001
	4 min	0,065 ± 0,006	1,130 ± 0,065	<0.0001

On the contrary, when PRP was layered upon the cells, statistically significant mineralization was observed in the absence of photostimulation ($p<0.001$) and the laser stimulation was able to further increase mineralization only when the

fluence was equal to 5 J/cm² delivered in 2 minutes (alizarin, mM: 5 J/cm² -1 min=0,712 ± 0,117; 5 J/cm² -2 min= 1,129 ± 0,127* , 5 J/cm² -4min= 0,769 ± 0,081; p<0.05), and 10 J/cm² in 4 minutes. (alizarin, mM: 10 J/cm² -1 min=0,847 ± 0,043; 10 J/cm² -2 min=0,753 ± 0,050, 10 J/cm² -4min= 1,130 ± 0,065; p<0.05) (Fig.16).

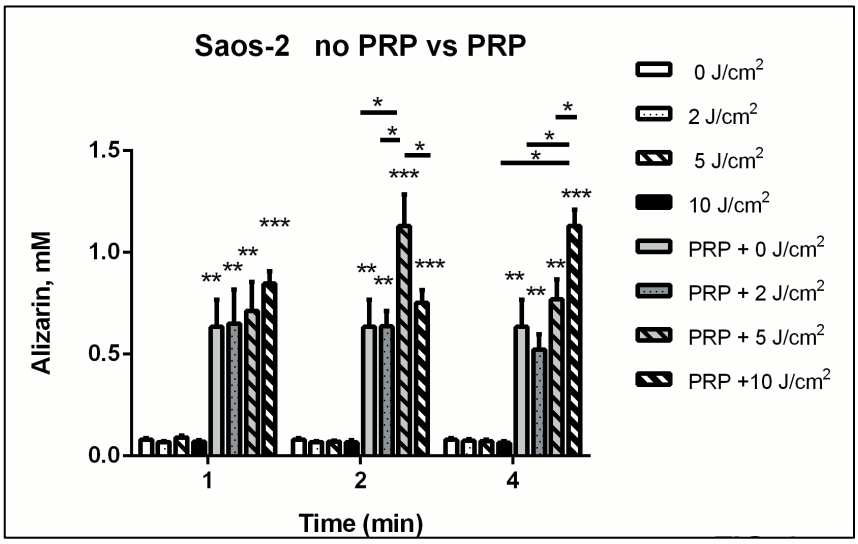

Figure 16: Differentiation of Saos-2 cells in the presence or absence of PRP with or without laser iradiation. X-axis: time of irradiation (minutes); y-axis: mineralization measured as Alizarin red concentration.

DISCUSSION

During culture with appropriate mineralizing conditions, Saos-2 cells reproducibly synthesize a bone-like mineralized matrix and temporally express mature osteocyte marker genes[42].

These characteristics make Saos-2 an attractive model with which to investigate the osteoblastic differentiation pattern. Therefore, we chose this cell line to

investigate, *in vitro*, the effect of photobiomodulation on cell growth and osteoblastic differentiation.

In a previously published study, we were able to evaluate the absorption of a red-light laser with a 645-nm wavelength in the oral cavity tissues of swine. We showed that the laser beam can reach the periosteum which is lined with osteoblastic cells[36].

The protocols were designed to mimic an *in vivo* situation of a post-extraction alveolar socket to the greatest extent possible. Immediately after the lesion of tissues, the alveolar socket is filled with blood, followed by subsequent clotting. Platelet activation is an important trigger of the healing process through the secretion of growth factors and cytokines. Therefore, we analyzed the effects of photobiomodulation on Saos-2 cells, plated in 5 mm diameter wells and covered, or not, by PRP, adopting a culture medium with a very low concentration of FBS (0.1%). This low FBS concentration was unable to stimulate either growth or differentiation, measured by Alizarin red assay, in our cell model.

Saos-2 cells are derived from an osteogenic sarcoma, and our observations suggest that, in the absence of growth factors, cancer cells are not induced to proliferate by 645 nm laser illumination with the fluences tested thus far.

PRP, as expected, and as is in line with what has already been reported, induced cell growth and mineralization, measured as an osteoblastic differentiation index, in Saos-2 cells [43], [44].

When growth factors and cytokines were present, we observed that both cell growth and differentiation were further stimulated only when a defined amount of energy was delivered.

Taken together, these data might suggest a novel action of photobiomodulation. If we had not detected any effects on growth or differentiation in the absence of PRP, it would have meant that the illumination of cells was not able to fulfill the promotion of these actions. However, as we measured the effects only in the presence of growth factors, it suggests that the laser beam could interact with some pathways triggered by growth factors i.e., inducing the expression of growth factor receptors or other key proteins of growth factor signal transduction. In addition, the stabilization of growth factor-receptor binding could be hypothesized, as only a specific amount of energy was found to be effective.

With the experimental protocol employed, we layered the PRP on top of the Saos-2 cells on day 1, and, on every other day of the medium replacement, PRP was progressively washed out, as happens in vivo during the post-extraction healing process. This confirms the power of PRP, whose effects were observed throughout our experiment, since it seems that its effects persist beyond its physical presence. However, we can exclude neither the binding of platelet growth factors to the extracellular matrix synthesized by the Saos-2 cells nor the synthesis of new growth factors by activated Saos-2.

The role of photobiomodulation on osteoblastic cells is not completely understood, although many of the mosaic tiles are in place. A recent review by Deanna and coll., focused on photobiomodulation and osteoblastic cells, found 1439 studies published in the past 20 years. Of these,1374 papers turned out to be on cell models other than osteoblasts, and only 22 of them fulfilled the criteria of the review. Only six papers used Saos-2 as the cell model[45]. Nevertheless, the studies did not use the same wavelength. For some of them, the principal mechanism elicited by light was ascribed to excitation of heat (or light)-gated ion channels, especially with long wavelengths (980 nm), but cytochrome-c activation seems to be the principal transducer for shorter wavelengths (630-710 nm).

Chant and coll. reported an increased proliferation and differentiation of MC3T3-E1 cells when illuminated by LED devices without differences if 630±5 nm or 810±10 nm were used[46].

In our study, we utilized a 645 nm laser with an energy density from 2 to 10 J/cm^2. Aleksic and coll. reported having proliferative effects without cytotoxicity in the MC3T3-E1 osteoblastic cell line within the same range of fluence[47].

Tani et al. reported an increased proliferation of Saos-2, cultured with 10% of FBS when irradiated with a 635 nm laser[48]. Along with proliferation, these authors described the increased expression of Akt and its phosphorylation,

suggesting a possible link between Ca^{2+} influx through the Transient Receptor Potential Canonical (TRPC)-1 membrane calcium channels and Akt activation.

Our results support this hypothesis, given that phosphatidylinositol 3-kinase (PI3K)-Akt trail is a signal transduction pathway that stimulates proliferation and differentiation in response to growth factor signals such as PDGF, IGF, and EGF. Akt, in turn, increases the abundance of TGF-β receptors at the cell surface, intensifying TGF-β responsiveness[49].

In Saos-2 cells, PRP promotes proliferation through the release of platelet-derived growth factor-AB (PDGF AB) and differentiation through TGF-β1[44]. If TGF-β receptors are abundant on the cell membrane, it is reasonable that it could result in a signal amplification in target cells. At the moment, this is pure speculation, and it needs to be addressed with targeted experiments. Nevertheless, it seems to fail to explain why there is no proliferation in the absence of growth factors even though Akt phosphorylation should increase, as Akt phosphorylation is only one of the signal transducers of the growth factor pathways.

The combination of photobiomodulation and PRP can lead to a statistically significant increase in both prolifera- tion and differentiation rates. The laser applications of 5 J/cm^2 delivered in 2 min and of 10 J/cm^2 in 4 min were proven to be the most effective. The results of this study underline the importance of the amount of energy delivered to the tissue; therefore, the laser instruments

utilized by the practitioners should provide this information to the users. Further studies will be needed to explain the MOA that PRP in combination with the laser at the appropriate settings produces on tissue to fully understand its potential to promote healing.

This first study represented the foundations for the second *in vitro* study (conducted during the second year) on two additional cell lines (HOS and U-2 OS) from osteosarcomas to verify the possible effects of LLLT on neoplastic cell growth.

PART II - IN VITRO STUDY ON HOS AND U2OS

MATERIALS AND METHODS

The following cells lines were selected for this *in vitro* study:

A) HOS (ATCC CRL-1543): derived from human osteosarcoma; these cells show flat morphology, low saturation density, low soft agar plating efficiency and are sensitive to chemical and viral transformation.

B) U-2 OS (ATCC HTB-96): derived from human osteosarcoma; unlike HOS, U-2 OS are characterized by strong alterations in the number of chromosomal sets, it is described differently depending on the source (even in mutual disagreement), from "hypodiploid" to "hypertriploid" chromosomal count.

Cells were seeded into 96-well plates at a concentration of 5000 cells / well and were kept for the entire duration of the experiment (14 days) in an incubator at a temperature of 37 ° C, at 5% CO2.

The medium changes were performed every other day, before laser treatments.

Cells were seeded in alternating rows and columns, to prevent any possible cross radiation from other neighboring wells.

Wells without cells were filled with medium only to facilitate thermal maintenance during irradiation outside the incubator. Also, to minimize temperature variations inside wells, rows and peripheral columns adjacent to edges of the plate did not contain seeded cells.

All 96-well plates were placed in customized metal casts to increase thermal isolation.

The study was set up in as the study conducted on Saos-2 cells: irradiation took place inside a vertical laminar flow hood (Biohazard Aura - B4).

The laser tip with a 0.5 cm diameter was fixed and anchored to a semi-articulated metal arm and its position was kept fixed throughout the duration of the experiment. At irradiation time, seeded 96-well plates were positioned on a fixed support, parallel to the laser tip; distance between the laser tip and irradiated well was kept constant.

The photobiomodulation was performed with the same laser with a wavelength of 645 nm used in the experiment on Sos-2 with.

The following table shows 9 experimental conditions investigated:

no PRP	no PRP	no PRP	no PRP	PRP	PRP	PRP	PRP	PRP
CTRL -	5 J/cm2 2’	10J/cmq 4’	CTRL +	CTRL -	5J/cmq 2’	10J/cmq 4’	2J/cmq 2’	10J/cmq 2’

For statistical evaluation, each experimental condition was replicated for 3 wells.

When expected, the PRP was placed at the beginning of the experiment to cover the cell monolayer and it had a concentration of 2691x103 platelets / ml, it was obtained by centrifugation at 2000 rpm for 5 'and subsequently "gelled" by

adding 200 µl of defibrinated plasma and 15 µl of calcium gluconate (100 mg / ml stock solution) per ml of PRP.

Laser irradiation was performed every other day for a total of 6 photobiomodulation.

Cell replication and calcified matrix deposition were evaluated by Alamar Blue and Alizarin Red assays, respectively. The vitality test with Alamar Blue was performed before each medium change, while the Alizarin Red test was performed at the end of the experiment.

Each treatment condition, indicated in the previous table, was "duplicated" so that it was characterized by the presence of a maintenance medium where plates were used for the execution of the Alamar Blue assay and a permissive medium for differentiation where cells were used for the Alizarin Red assay.

Medium's composition used is shown below:

- for Alamar Blue assay

medium (except ctrl +): DMEM low glucose; glutamine 2 mM; FBS 0,1%; streptomycin/penicillin 1X;

CTRL + : DMEM low glucose; glutamine 2 mM; FBS 10%; streptomycin/penicillin 1X.

- for Alizarin Red assay

medium (except ctrl +): DMEM low glucose; glutamine 2 mM; FBS 0,1%; streptomycin/penicillin 1X; proline 4 µg/ml; ascorbate 100 µM; β-glycerophosphate 2 mM;

CTRL + : DMEM low glucose; glutamine 2 mM; FBS 10%; streptomycin/penicillin 1X; proline 4 µg/ml; ascorbate 100 µM; β-glycerophosphate 2 mM.

Results were analyzed with the software GraphPad Prism 6.0.

RESULTS

Results are shown in following graphics:

Alamar Blue assay on HOS cell line: Figures 17 and 18.

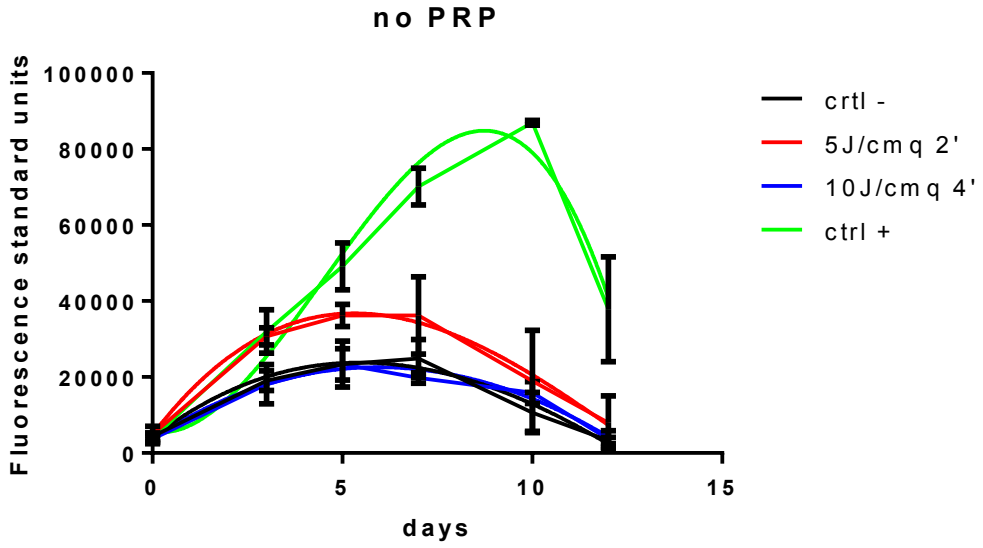

Figure 17: Proliferation's rate assessment of HOS cell line in absence of PRP.

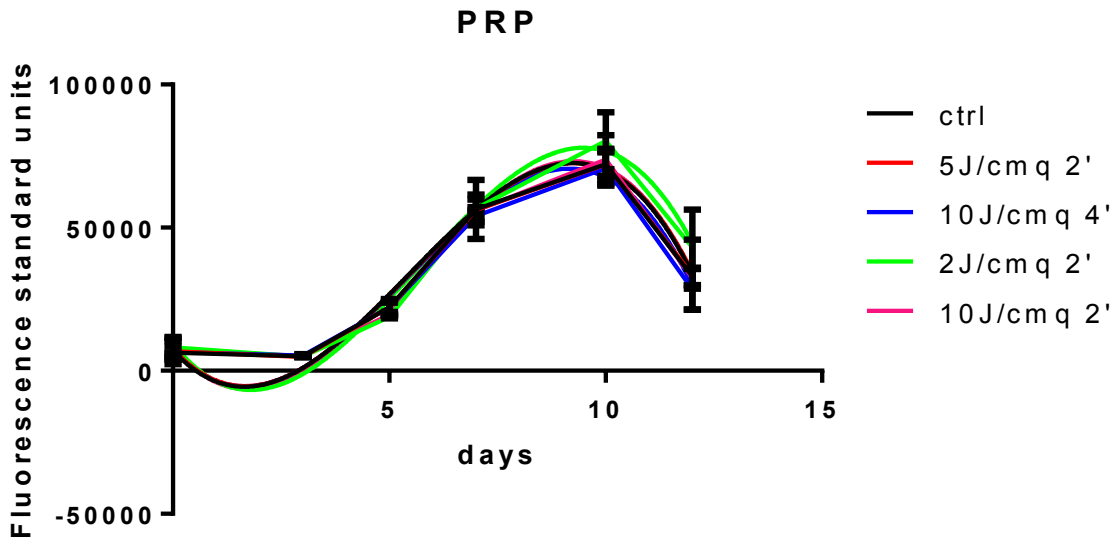

Figure 18: Proliferation's rate assessment of HOS cell line in presence of PRP.

Alamar Blue assay on U2-OS cell line: Figures 19 and 20

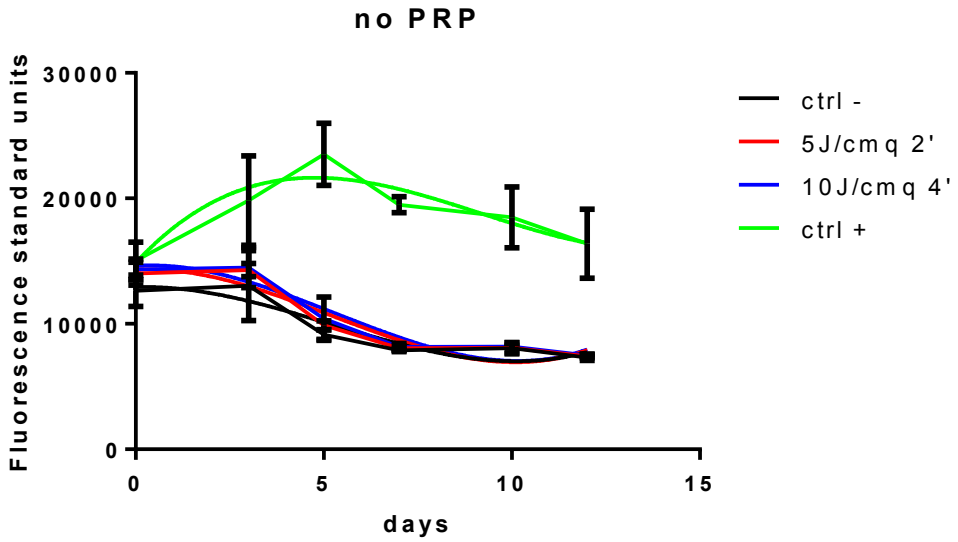

Figure 19: Proliferation's rate assessment of U2-OS cell line in absence of PRP.

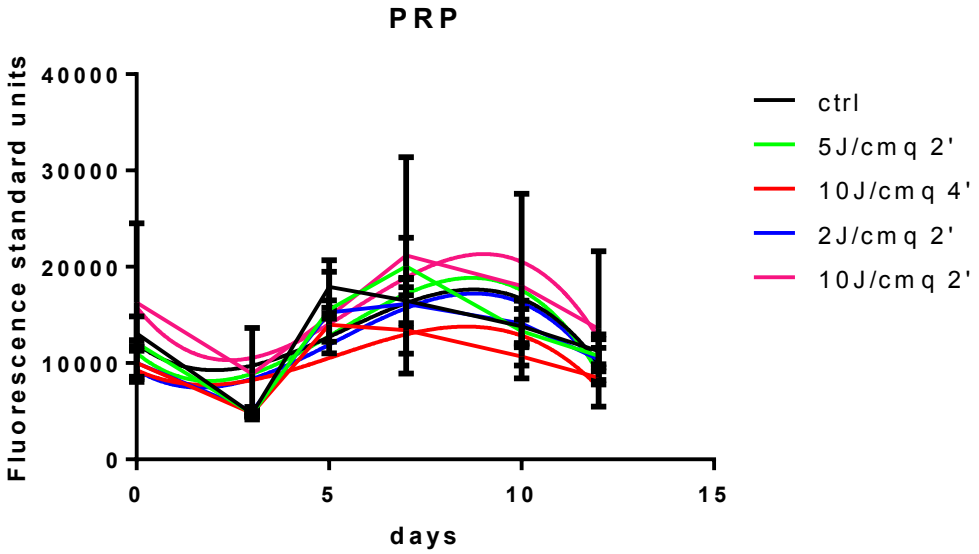

Figure 20: Proliferation's rate assessment of U2-OS cell line in presence of PRP.

Alizarin Red assay: Figures 21 and 22.

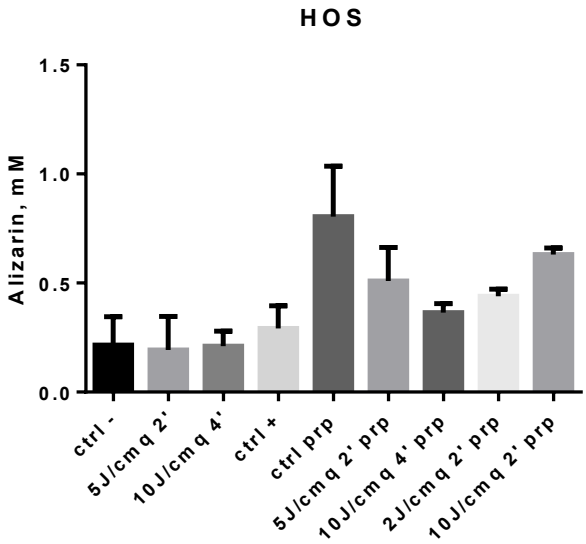

Figure 21: Differentiation rate assessment of HOS cell line.

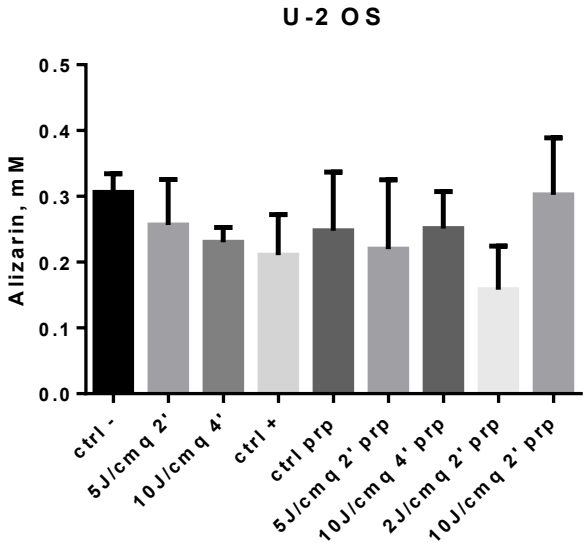

Figure 22: Differentiation rate assessment of U2-OS cell line.

DISCUSSION

Obtained data immediately highlighted the different behavior of the two cell types in response to same stimuli.

Considering separately data obtained in the presence of PRP, we took into consideration both cell types with CTRL + condition (without PRP): the proliferation's rate is always significantly higher ($p < 0.01$).

Concerning HOS: the analysis of cell proliferation shows its substantial independence from the laser treatment in the presence of PRP while, among the treatments performed without PRP, the treatment with 5 J / cmq for 2' in particular at day 5 showed a statistically significant difference ($0.1 < p < 0.05$).

Regarding U-2 OS model, on the other hand, no variation was shown according to treatments, regardless of the presence or absence of PRP.

In Figures 17 and 18, as in Figures 19 and 20, comparison between presence and abscence of PRP is shown: the presence of PRP influenced statistically significantly cell's proliferation in both HOS and U-2OS.

Calcium deposition was constant regardless of laser treatment for the U-2 OS cell model while for the HOS cell line data showed a tendency to deposition in the presence of PRP.

Considering the difference in the experimental results obtained from these models, both between them and in comparison to the previous Saos-2 model, it is evident that the 3 cell lines, despite their common "osteoblastic nature", do not show the same behavior when subjected to the same treatment.

The 3 cell lines, characterized by a common oncologic nature, in the presence of a large amount of growth factors (such as in the PRP) seem to be induced to an increased cell proliferation.

We could hypothesize a new mechanism of action for which the energy delivered is able (in some way) to stabilize the link established between one or more unidentified growth factors present in the PRP and its related receptors.

The peculiarity linked to the different expression of receptors in these models could explain which of these receptors (and therefore growth factors) is actually responsible for the induction of a higher deposition of calcifications as well as the different proliferation' rates observed in all 3 experimental models.

It was also observed (both in these and in the previous *in vitro* study) a generalized increase in proliferation' rate induced by the presence of PRP, regardless of the laser photobiomodulation treatment; this finding could be explained by the stimulation of the Akt pathway which follows an induction due to growth factors such as EGF, PDGF and IGF and stimulates cell proliferation and differentiation.

Furthermore, the conditions of the study with a concentration of FBS equal to 0.1% may further corroborate our hypothesis: it is in fact indicated in the literature as, in particular IGF-1, is fundamental for the survival and proliferation of osteoblastic cells in the absence of serum and how its receptor is present in the three investigated models (as mentioned in Kappel et al. in Human Osteosarcoma Cell Lines Are Dependent on Insulin-like Growth Factor I for in Vitro Growth [50]).

The different response to treatments, which showed the first Saos-2 model as more sensitive to treatments (at least in terms of calcified matrix deposition), compared to the HOS and U2-OS cell models, could be explained by the different expression of IGF-1 by the three models studied.

PART III - IN VIVO THERMAL EVALUATION DURING PHOTOBIOMODULATION WITH A 980 NM DIODE LASER ON DIFFERENT CUTANEOUS PHOTOTYPES

As previously stated, in vitro and clinical studies have demonstrated four main actions of laser photobiomodulation:

1) analgesic effect;

2) anti-edema effect;

3) decontaminating effect;

4) effect of inhibition or activation of intra-cellular processes.

Photobiomodulation is a characteristic of lasers with a wavelength between 600 nm and 1064 nm, this range is called "therapeutic window".

In international literature, all wavelengths with biostimulation or biomodulation activities in the oro-maxillofacial area are reported.

To achieve PBM, very low energy are delivered for long application's times.

The mechanism of action underlying LLLT is probably of photochemical nature and yet to be completely understood [2].

The primary photoaceptors may be found in the mitochondrial respiratory chain or at the level of the cell membrane. Cellular photoreceptors are considered to be cytochromophores such as endogenous porphyrins and molecules of the respiratory chain such as cytochrome c-oxidase.

The absorption of laser light by the components of the respiratory chain causes a short-term activation of the respiratory chain itself and the oxidation of the NADH, causing changes in the redox state of the mitochondria and cytoplasm. The activation of the electron transport chain determines an increase in the membrane potential of the mitochondria and an increase in the production of ATP, these cause the alkalinization of the cytoplasm and, as a final consequence, the triggering of the synthesis of nucleic acids and the acceleration of cell metabolism [31].

It has been hypothesized that the action of the LLLT may also take place through the induction of the formation of "singlet oxygen", a form characterized by high energy and high reactivity. The LLLT determines an increase in the amount of mRNA at the base of the synthesis of type I and type III collagen and therefore a stimulating action on the production and repair of mucousa and bone tissue.

LLLT may also stimulates cell proliferation by inducing cell cycle regulatory proteins and cell differentiation.

No studies, to date, have clearly stated a pathway in which laser light involvement is clearly explained, so PBM still remains an interesting subject of study since biological effects have been widely observed in all medical branches, not only dental, but not fully explained. Reported clinical benefits of PBM have been observed but, up to date to the limit of our knowledge, no studies investigated temperature variation during PBM.

The purpose of the present study was to assess if, given a certain Fluence value, Power Density (PD) variations during PBM sessions administered on patients with all of the six Fitzpatrick phototypes can induce significant changes in skin temperature.

MATERIALS AND METHODS

To conduct this in vivo study twelve subjects, six females and six males, with a mean age of 40 years (range: 19-70 yo) were recruited. Our sample was created, so that each Fitzpatrick skin phototype would have been tested, with two subjects for each phototype. Pregnant or breastfeeding women, individuals undergoing natural or cosmetic tan, patients with a known or suspected history of malignant skin disease and subjects with previous exposure to ionizing radiation and/or chemotherapy were excluded from the study. Only healthy individuals with hairless skin and no skin patches, scars, tattoos, acne or other forms of skin infection, were considered eligible for participation. To maximize data collection and double irradiation sites, the laser application was performed on both cheeks for each participant. Phototypes were selected through comparison with Fitzpatrick skin type scale [51], as shown in Figure 23.

Figure 23: Fitzpatrick skin type scale and corresponding patients.

Age, sex and tan history were collected and recorded for each patient. Site preparation was carried out as follows: a pH-balanced cleanser was used to delicately wipe each skin site, thus removing any residual of creams, ointments, make-up, and aftershave lotions. Scrubbing was avoided in order to prevent superficial vasodilation, which could lead to a distortion of temperature. Patients were verified to be without fever.

Raffaello DMT is equipped with a software able to calculate autonomously the irradiation time based on the fluence and Power Density set by the clinician. Moreover, the program gives the possibility to modify one or more parameters while keeping the remaining unchanged.

For this study, a 980 nm Diode laser was used (Raffaello DMT Italia, Lissone-Italy, year of manufacture: 2014), CW, connected to a designated and collimated PBM handpiece (spot size 0.5 cm^2) kept perpendicularly 2 mm far from each skin site, with an off-contact approach.

Therefore, for the purpose of this study, in line with WALT guidelines [52] our laser was set with a fixed energy density of 4 J/cm^2 and three increasing values of PD:

Protocol 1: PD: 0.2 W/cm^2 (200 mW/cm^2) for 20 s;

Protocol 2: PD: 0.4 W/cm^2 (400 mW/cm^2) for 10 s;

Protocol 3: PD: 0.6 W/cm^2 (600 $mW/cm^{2)}$ for 6,6 s.

Subjects and researchers put on appropriate laser safety glasses for the duration of the testing.

Skin site was chosen from the central portion of the right cheek and the left cheek, with a surface of 1x1cm^2 each. After the delicate skin wiping aforementioned, each one of the six sites were covered with a preformed paper template, and exposed to PBM with "point-by-point technique", for a total of four points in each skin site.

The following 8-phase scheme was carried out for each patient:

PROTOCOL 1, on right cheek, repeated for 3 times, with time interval of 5 min between the sessions;

PROTOCOL 1, on left cheek, repeated for 3 times with time interval of 5 min between the sessions;

PROTOCOL 2, on right cheek, repeated for 3 times, with time interval of 5 min between the sessions;

PROTOCOL 2, on left cheek, repeated for 3 times, with time interval of 5 min between the sessions;

PROTOCOL 3, on right cheek, repeated for three times, with time interval of 5 min on between the sessions;

PROTOCOL 3, on left cheek, repeated for three times, with time interval of five minutes on left cheek between the sessions.

Thermographic examination was performed by thermal camera (Fluke Ti450 Infrared Camera) kept 25 cm far from skin, according to the manufacturer instructions, with the aim to prevent any interference with the hypothetical thermal changes caused by PBM.

Under a steady room temperature of 22 °C, and bearing in mind a thermal relaxation time of 0.2-1 ms for skin, each skin site had thermograms taken in three specific moments:

- before PBM (T_0),
- right after the end of PBM (T_1),
- 30 seconds after the end of PBM (T_2).

RESULTS

T_0, T_1, T_2 were measured for each of the three sessions of Protocol 1, Protocol 2, and Protocol 3, amounting to:

- 9 temperature measures for each Protocol;
- 27 measures for each cheek;
- 54 temperature measures in total.

PBM sessions did not induce a significant increase of temperature in neither of the three protocol tested, nor it created significant differences among the six Fitzpatrick phototypes, with no complaint of heating coming from the 12 individuals enrolled in the experiment.

Table, 4, 5 and 6 report the average T_0, T_1, and T_2 on each phototype, for each of the three protocols.

Table 4

Phototype	Protocol 1 - T_0	Protocol 2 - T_0	Protocol 3 - T_0
I	31. 76°C	31.89°C	32.10°C
II	32.23°C	32.46°C	32.61°C
III	32.19°C	31.97°C	32.12°C
IV	32.90°C	33.07°C	33.21°C
V	34.15°C	34.19°C	34.25°C
VI	32.34°C	32.17°C	32.11°C

Table 5

Phototype	Protocol 1 – T_2	Protocol 2 -T_2	Protocol 3 - T_2
I	31.81°C	31.92°C	32.19°C
II	32.27°C	32.55°C	32.71°C
III	32.21°C	32.01°C	32.22°C
IV	33.02°C	33.19°C	33.3°C
V	34.24°C	34.30°C	34.34°C
VI	32.34°C	32.21°C	32.05°C

Table 7 and associated following Figure summarize the average increase of temperature caused by PBM [$\Delta(T_1-T_0)$]. Table 8 and associated following Figure and the average decrease after 30 seconds since the conclusion of PBM [$\Delta(T_2-T_1)$].

Table 6

Phototype	Protocol 1 - T_1	Protocol 2 - T_1	Protocol 3 - T_1
I	31.91°C	32.07°C	32.32°C
II	32.39°C	32.68°C	32.89°C
III	32.29°C	32.19°C	32.41°C
IV	33.12°C	33.38°C	33.51°C
V	34.38°C	33.43°C	34.51°C
VI	32.57°C	32.43°C	32.38°C

Table 7

Phototype	Protocol 1 - $\Delta(T_1-T_0)$	Protocol 2 - $\Delta(T_1-T_0)$	Protocol 3 - $\Delta(T_1-T_0)$
I	+0.15°C	+0.18°C	+0.22 °C
II	+0.16°C	+0.22 °C	+0.28 °C
III	+0.1°C	+0.21°C	+0.29°C
IV	+0.22°C	+0.31°C	+0.3°C
V	+0.23°C	+0.24°C	+0.26°C
VI	+0.23°C	+0.26°C	+0.27°C

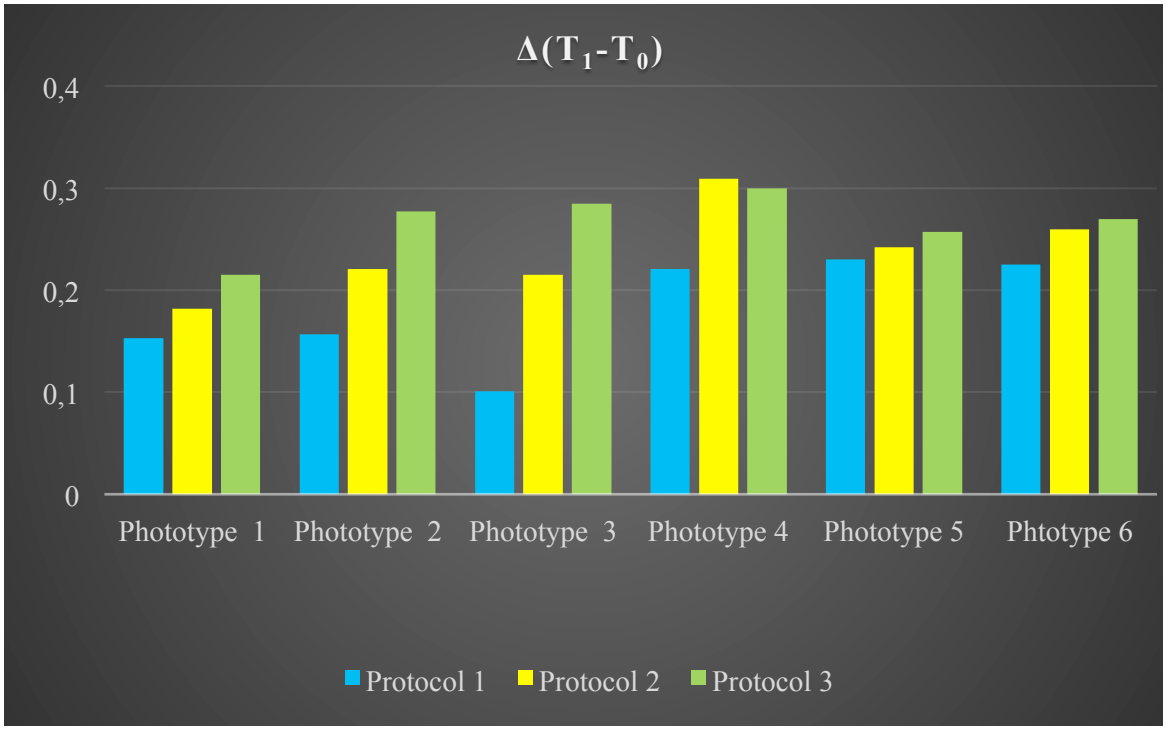

Table 8

Phototype	Protocol 1 - $\Delta(T_2-T_1)$	Protocol 2 - $\Delta(T_2-T_1)$	Protocol 3 - $\Delta(T_2-T_1)$
I	-0.10°C	-0.15°C	-0.13°C
II	-0.12°C	-0.13°C	-0.18°C
III	-0.08°C	-0.18°C	-0.19°C
IV	-0.1°C	-0.19°C	-0.21°C
V	-0.14°C	-0.13°C	-0.17°C
VI	-0.23°C	-0.22°C	-0.33°C

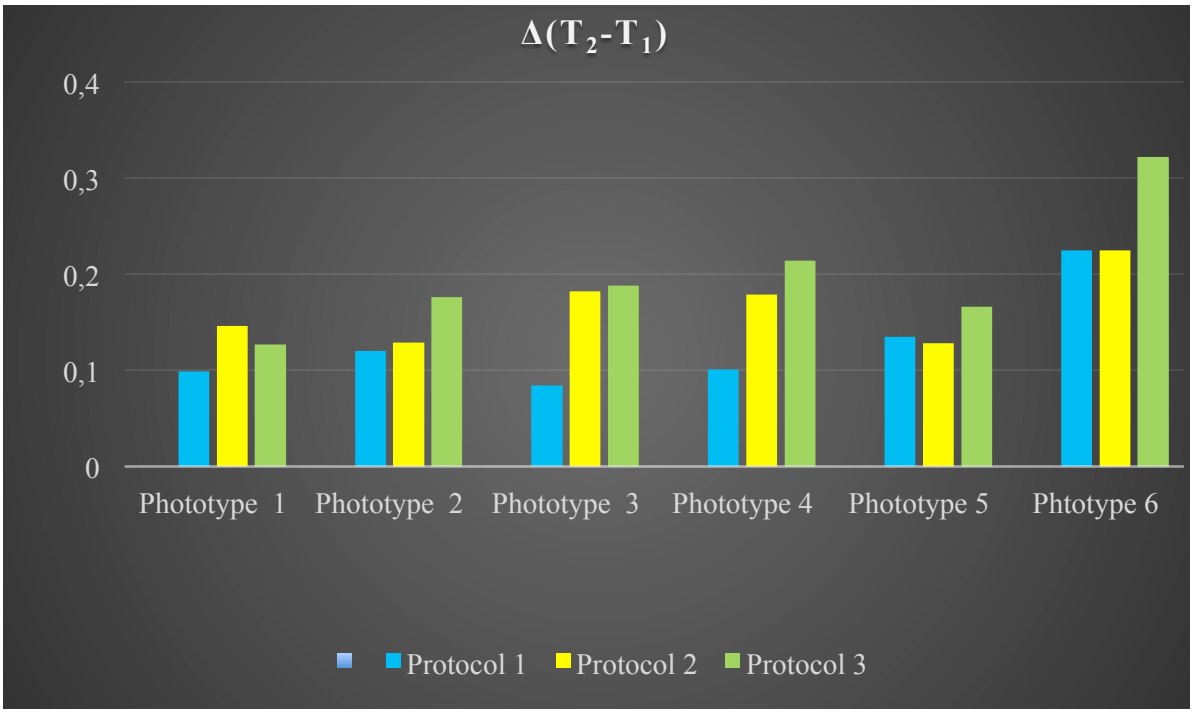

DISCUSSION

Our study showed no significant differences in temperature measures within the same phototype, during protocol 1, 2, and 3, with minimal temperature excursions between pre-PBM, PBM and post-PBM, as well as between the six phototypes.

Moreover, left cheeks showed lower baseline temperature, when compared to the contralateral side, although a PBM session was already conducted on the right cheek.

These data seem to be in contrast with the results by Japanese Authors in the first years of 2000, who reported an interesting increase of temperature on the left side of the face, after CO_2 irradiation of the skin of right TMJ [53], explained through a central nervous system-mediated phenomenon called vasodilator reflex, according to which heating on one side of the body, i.e. a limb, could induce an enhancement of circulation on the opposite side.

However, such difference may rely also on the different laser device and the different parameters deployed.

With regards to the non-significant differences detected between pre-PBM and post-PBM in all phototypes, our results seem to be aligned with most of the previous literature on thermal effects of diode laser therapy [54] [55] [56], and in striking contrast with the +22.3 °C increase of temperature reported by Joensen [57], where 8 dark skin patients asked also for laser treatment to stop, because of the distressing amount of heat perceived.

The present study carries some limits: the number of subjects recruited is small, and only three power densities have been tested (0.2 cm^2; 0.4 W/cm^2; 0.6 W/cm^2).

On the other hand, there are some merits to the present work: to the best of our knowledge, no other studies have been published concerning the thermal effects of a 980 nm Diode laser, with most of the forty-two studies found in literature on usage of Diode among Fitzpatrick phototypes focusing on 800 nm, 810 nm, and 1450 nm wavelengths.

These three wavelengths alone, in fact, have been tested in more than half (26 out of 42) of all of the studies.

In addition, none of these studies carried out a similar protocol where different Power Densities were to be tested keeping fluence unchanged.

More importantly, almost no study focused their efforts and aims on comparing the spectrum of therapeutic outcomes and/or side effects between the different phototypes enrolled, with few exceptions.

In this sense, 810 nm diode for hair reduction lead to no complication for individuals with darker skin in the paper by Agarwal [58], showing best results in phototype III in the study published by Sadick [59].

Concerning the reliability of diode laser on acne, Taub [60] noticed no difference in improvement after usage of 915 nm diode for acne scars between phototype II and V, whereas Jih [61] and Chua [62] case-series proved an overlapping safety in treating facial acne with 1450 nm wavelengths, with no adverse effects among patients of phototypes IV-VI.

Apart from the aforementioned studies, in the remaining articles the subgroups of patients with different Fitzpatrick phototypes are usually specified when describing the sample selection process and/or its main features but, ultimately, no exact distinction are described in the results concerning the differential profile of efficacy or risks of Diode laser for each one of the phototypes involved.

A better study design should consider not only a larger sample, but also an even more insulated environment, preferably with no windows at all, in order to minimize the infinitesimal variations of temperature, which might come from leaking window-wall interfaces.

Additionally, a more user-friendly remote-controlled thermal camera could contribute to the indisputability of the thermal calculations, so that no bias could descend from the most imperceptible movements or breathing of the clinician designated to measurement of temperature at T_0, T_1, and T_2.

In order to weigh the alarming results coming from Joensen [57], a wider range of fluences and power densities than the ones experimented in this work should be scrutinized, going gradually up from Low-Level-Laser Therapy to those fluences (>80 J/cm^2) belonging to High Fluence Low Power Laser Irradiation (HF-LPLI).

Only with this approach in mind, it will be possible to provide a reliable threshold of thermal safety for PBM.

The clinical utility of these investigations could be found in the prospect of providing safe-and-faster sessions of PBM, due to the inverse correlation between PD and irradiation time.

In oral medicine, such approach might be particularly needed among patients with bullous diseases or chemo-radiotherapy induced oral mucositis, who, notoriously, present difficulties in keeping the mouth open for too long.

In line with the vast majority of literature, our case-series showed no concerning thermal effects on the skin of subjects with all six Fitzpatrick phototypes undergoing PBM with low fluence and power densities, with no noticeable difference between light and dark skin individuals.

Further studies with larger samples, and wider range of parameters – 645/980 nm wavelengths, fluences and power densities higher than 4 J/cm^2 and 0.2-0.6 W/cm^2, respectively – are warranted to shed light on the controversial spectrum of thermal side effects of PBM.

Experimental setup might be improved with a thermostated room and a remote-controlled thermal camera to minimize thermic interferences.

PART IV - THERMAL EVALUATION AND ITS AUTOFLUORESCENCE CORRELATION: IN VIVO AND EX VIVO STUDY

Auto-fluorescence (AF) is a property possessed by every cell that exposed to a specific wavelength can absorbance or reflect with peculiar characteristics [63], [64].

Changes in autofluorescence reflect complex alterations to fluorophores in tissue and structural changes in morphology. These autofluorescence changes are caused by alterations in structure (i.e hyperkeratosis, hyperchromatin, and increased cellular and nuclear pleomorphism) and metabolism (concentration of flavin adenine dinucleotide-FAD and nicotinamide adeninedinucleotide-NADH of the epithelium and the composition of the collagen matrix and elastin of subepithelial stroma) [65].

The involvement of natural endogenous fluochromes which are located within the oral epithelium and the submucosa imply the excitement of target tissues with specific wavelengths (such as 375 and 440 nm) and the analysis of the emitted green light with a selective narrow-band filter [66].

AF of oral tissues and its direct examination has been proposed as a non-invasive visual tool for investigation of suspicious changes in oral mucosa.

AF has been used for early detection of pre-malignant and malignant oral lesions as a screening tool: the variation in emitted fluorescence can help to detect possible areas of oral dysplasia or oral squamous cell carcinoma that deserve further diagnostic investigation through biopsy sampling (which remains the gold standard for diagnosis) [67]; the use of AF has led to the improvement of diagnostic first level accuracy [68].

The usefulness of AF has also been shown during clinical evaluation between viable and non-viable bones in hard tissue surgery (such as osteotomy and margin revision in patients affected by Medication Related Osteonecrosis of the Jaw) [69].

Seen results during photobiomodulation obtained while carrying out this thesis work, it was decided to further investigate possible temperature variations related to tissue autofluorescence modifications also during cutting with different surgical instruments.

A previous work, in course of publication, had shown that the application of biostimulation on the skin of subjects with different phototypes did not lead to significant differences in surface temperature increase: our case-series (composed of two individuals / sample for each classified Fitzpatrick phototype) showed no concerning thermal effects on the skin of subjects with all six Fitzpatrick phototypes undergoing PBM with low fluence and power densities, with no noticeable difference between light and dark skin individuals.

A brief in vivo evaluation of variation in AF after PBM performed with a diode laser with a wavelenght of 970nm highlighted no difference in AF detected before and after biostimulation.

Figure 24 show 3 healthy patients that underwent PBM (970 nm, 0.5W, 10Hz, 5 minutes application) with corresponding AF pictures righte before (T1) ad after (T2) irradiation.

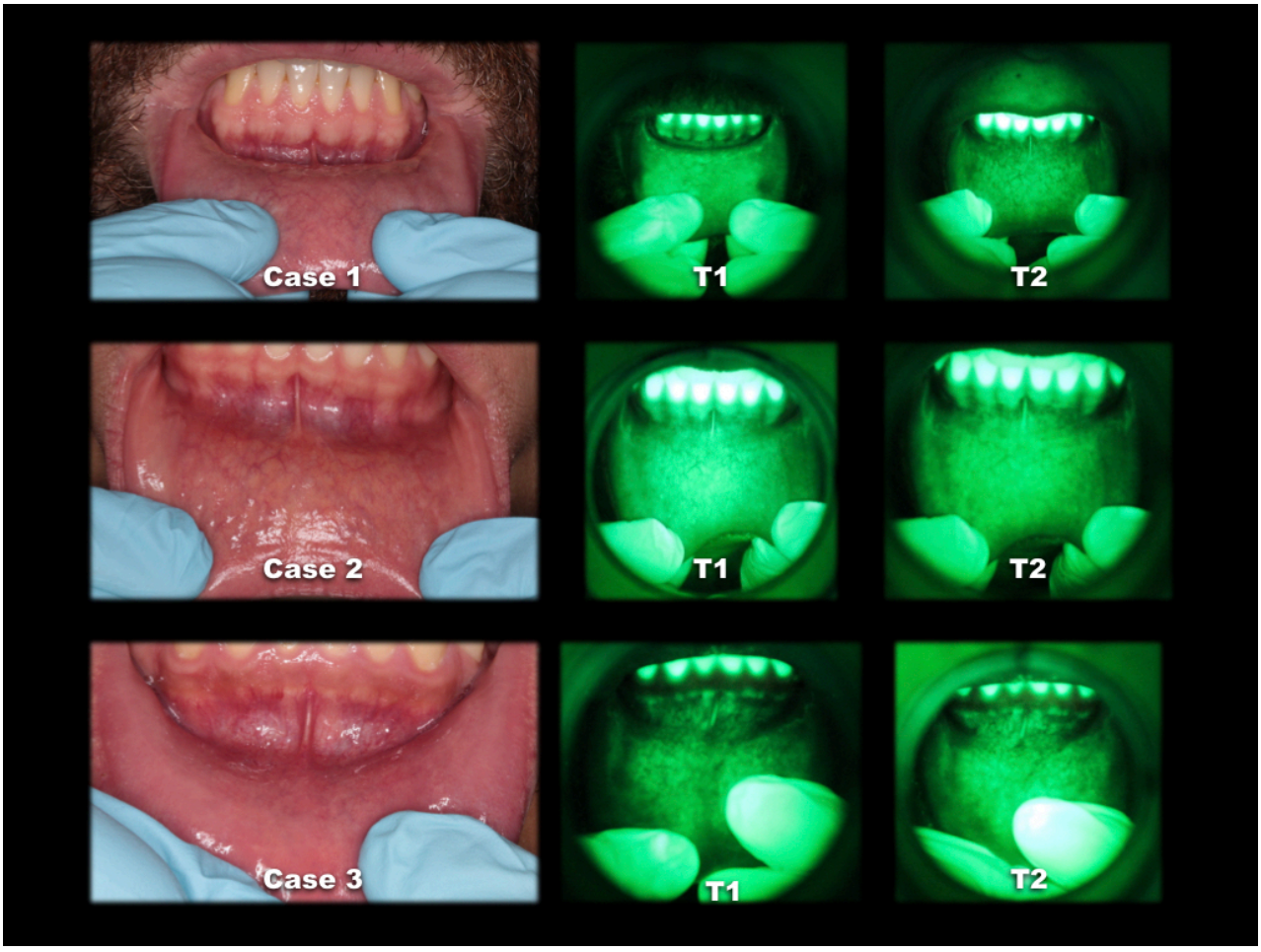

Figure 24: AF evaluation in 3 healthy patients before and after PBM.

Surgical techniques of soft and hard oral tissues highly benefited from new technologies such as the Quantic Molecular Resonance (QMR) lancet, the

Neodymium-doped Yttrium Aluminum Garnet (Nd:YAG) laser and the Erbium-doped Yttrium Aluminum Garnet (Er:YAG) laser.

Increasingly, these technologies replace scalpel, conventional electrosurgery and traditional rotary surgery instruments due to their proven advantages. Features as: reduction of the surgical time, more efficient bleeding control resulting in higher intra-operative visibility and improvement of postoperative course [3] with better Quality of Life score (QoL) are highlighted in numerous studies published in the literature.

The QMR lancet is a relatively new technology that applies high frequency waves to soft tissues. It is able to cut non-traumatic and to performe gentle coagulation. The cut is achieved by the explosion of infra-cellular and intracellular liquids, that resonate with a special frequency [70].

The use of lasers in oral surgery is strictly related to the specific affinity of their wavelength to different tissue molecular components.

Depending on the absorption rate within the visible and near infra-red spectrum, we can differentiate laser with hight affinity for hemoglobin (such as Nd:YAG laser) or for water (such as Er:YAG laser) [71].

Since water represent a major part of human cells, the action of Er:YAG laser on soft tissue is particularly effective and typically superficial; this type of laser is able to also induce ablation in hard tissues: the -OH group within hydroxyapatite constitute the target for 2940 nm wavelength [72].

The Nd:YAG laser with its affinity for hemoglobin is ideal for photocoagulation (even on deep lesions, as it is able to penetrate full thickness into oral tissues) and for surgery with simultaneous hemostasis, it can be used for coagulation after surgery performed with traditional instruments [73].

Both lasers and QMR, through different processes, induce a variation in the temperature of treated tissues [74].

The thermal rise of tissues during surgical incision, performed with other instruments rather than traditional cold blade scalpels, is not to be ignored by the operator and it must take into consideration first when choosing the surgical instrument and then throughout all the surgical act [75], [76].

This factor has to be taken into consideration while operating, particularly inside the oral cavity [77]: the proximity of noble structures such as nerves, arteries and veins of medium caliber and glandular structures must be acknowledged and considered in order to avoid temporary or permanent damage.

At the limit of our knowledge, few studies have been published in the literature regarding tissue's temperature variations and the interest in Infra-Red temperature detection has been shown in various medicine fields.

For example, infrared thermography has been studied for measurement and characterization of brown adipose tissue activation as a potential target for novel obesity, diabetes and metabolic disease treatments.

Patients affected by migraine and tension-type headache were screened through thermo scanning and Infra-Red imaging and it was possible to detect myofascial trigger points [78].

Also, the clinical significance of thermal detection and its analysis was used to highlight abnormal temperature distribution of soft-tissue tumors [79] and for the diagnosis of musculoskeletal injuries [80].

Furthermore, the infrared thermography and the monitoring of temperature changes during open heart surgeries led to accurate determination of the moment for electrode removal [75].

None of published studies investigated the possible correlation between temperature raise and AF variations.

This *ex vivo* study aimed to analyze and compare through the use of a thermal imaging camera and simultaneous detection of AF the possible correlation between temperature raise and auto-fluorescence.

Three different of most frequently used surgical tools were investigated (i.e. Er:YAG laser, QMR and Nd:YAG laser) on both soft and hard tissue samples.

Are temperature's variations associated with modifications of emitted fluorescence?

MATERIALS AND METHODS

Incisions were performed on chicken soft tissues sample (ST-A), liver soft tissues sample (ST-B) and swine rib hard tissue sample (HT) preserved at 4°- 8° temperature before the experiment.

All cuts were performed by the same operator, who was instructed to maintain constant pressure and cutting speed throughout the experiment.

The operator did not touch tissue samples in the area corresponding to where incisions were to be performed (during the positioning of samples nor during cutting) in order not to alterate the sample's temperature with body heat.

The operator was guided by a centimetric level to perform incisions of 4 cm of length.

Due to statistical reasons, 3 cuts for each instruments on each tissue samples were performed.

To imitate the surgical applications of investigated newest technologies: Er:YAG laser without water, QMR and Nd:YAG were used to performe 9 incisions on each soft tissue sample; while on hard tissues, a total 6 cuts were performed using Er:YAG laser with or without water irrigation.

Chosen instruments were set as follows:

- Er:YAG laser: 2940nm, SSP mode, R02, 235 mJ, 3.5W, 15 Hz [Figure 25 and 26]

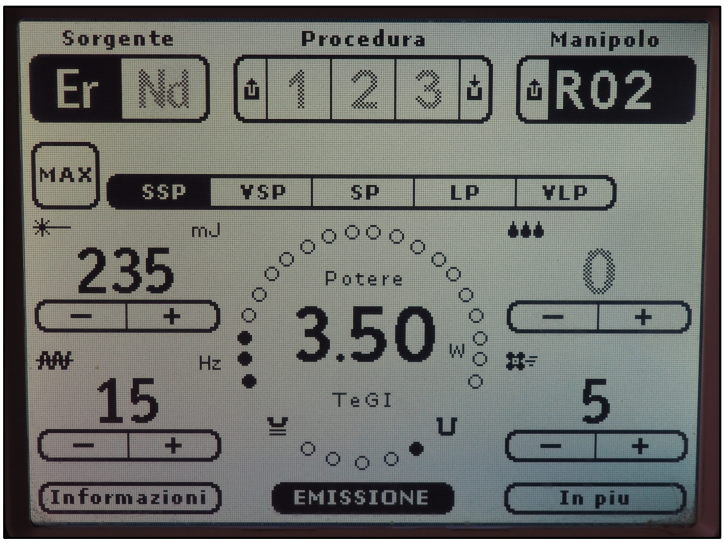

Figure 25: Er:YAG laser setting without irrigation.

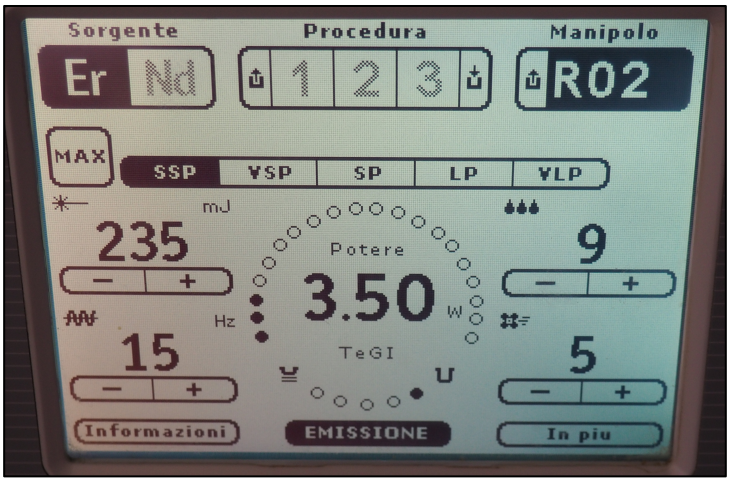

Figure 26: Er:YAG laser setting with irrigation.

- QMR: Cut 120W/400Ω [Figure 27]

Figure 27: Quantic Molecular Resonance lancet setting.

- Nd:YAG laser: 1064nm, VSP, fiber diameter 300µm, 3.75W, 75Hz [Figure 28].

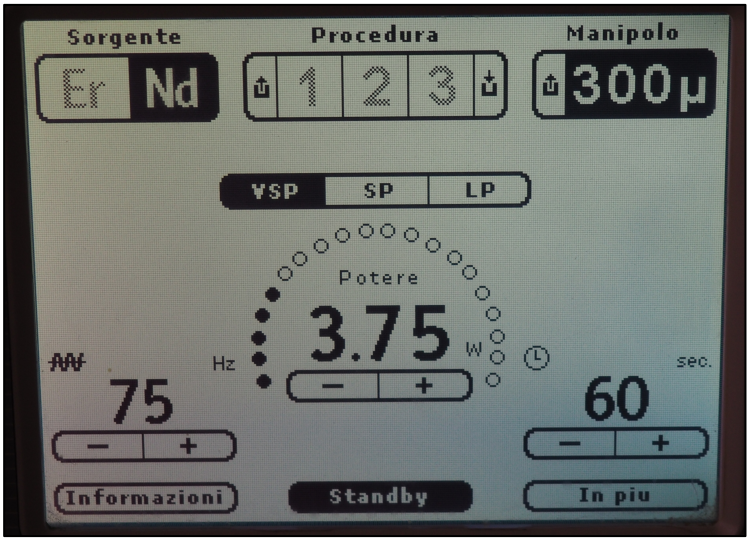

Figure 28: Nd:YAG laser setting.

The thermographic measurements were recorded with an infrared reading thermo-camera (Fluke TI300+, 320x240 pixel, Fluke Italia srl) positioned on a fixed static support at an angle of 45° to the target tissues.

Emissivity was set as 1.00; transmission was set as 100%; background temperature was detected previous the experiment and maintained constant at 26.8°C.

All temperatures were recorded in Celsius degrees (°C); the thermo-camera was set to automatically scan:

right before performing the cut (T0)

right after the cut was completed (T1)

after 30 seconds that the cut was completed (T2).

Highest and lowest temperature values in each frame were extrapolate and analyzed.

Fluorescence was stimulated through irradiation with a blue–violet light (410–30 nm wavelength) using the VELscope® system (LED Medical Diagnostics, Inc, Barnaby, BC, Canada). This is a medical device approved in 2006 by the US Food and Drug Administration as a support tool for the implementation of oral mucosa examination.

Frames were acquired immediately after the automatic thermo-camera detection.

Distance to the target tissue was maintained constant.

Corresponding scans acquired with the thermo-camera and Velscope were matched as shown as example in Figure 29 and Figure 30; noticeable variations in paired frames were highlighted.

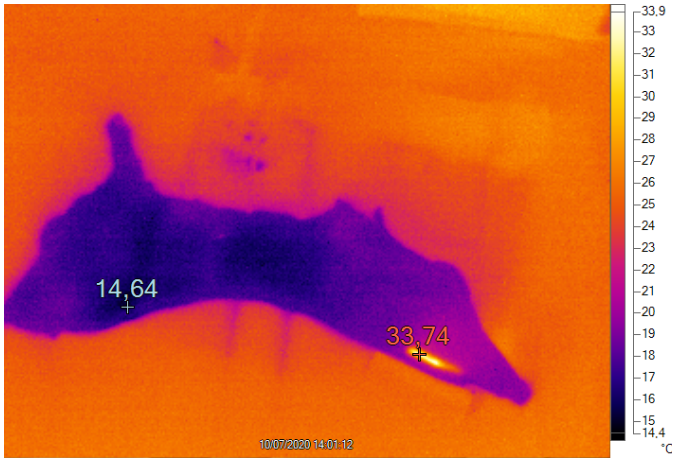

Figure 29: Example of matching between thermo-camera frame and Velscope frame: temperature scan.

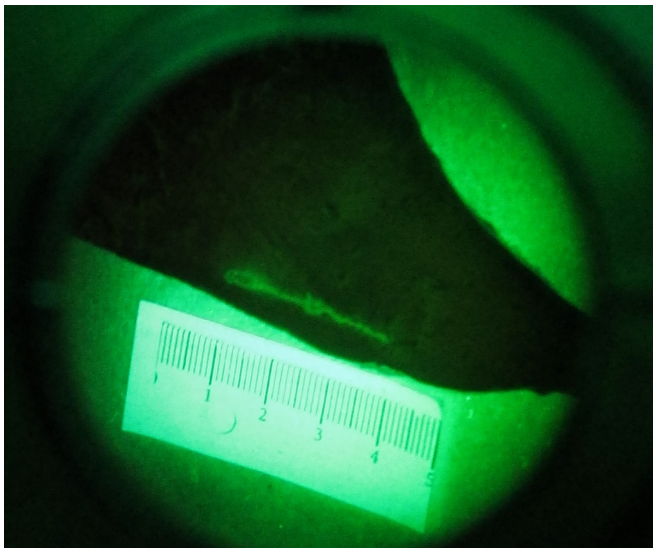

Figure 30: Example of matching between thermo-camera frame and Velscope frame: AF scan.

RESULTS

A total of 36 frames for hard tissue samples (HT) and 108 frames both for soft tissue samples (ST-A and ST-B) and were paired and analyzed.

Temperature's values are reported in following 8 Tables in Celsius degrees (°C). Highest values without *(*)* symbol were detected to be outside the tissue sample. Highest values with *(*)* symbol were detected to be on the tissue sample (where the cut was performed).

Er:YAG laser w H2O	T0 (°C)		T1 (°C)		T2 (°C)	
	lowest	*highest*	*lowest*	*highest*	*lowest*	*highest*
1st cut	17,52	34,19	17,98	33,32	18,01	26,77
2nd cut	18,58	34,85	19,43	35,07	18,35	26,16
3rd cut	18,7	34,96	18,59	33,79	18,47	27,38
Er:YAG laser w/o H2O	T0 (°C)		T1 (°C)		T2 (°C)	
	lowest	*highest*	*lowest*	*highest*	*lowest*	*highest*
1st cut	14,24	33,31	14,17	48,86*	14,79	28,01
2nd cut	14,82	27,04	15,27	26,29	15,05	27,07
3rd cut	14,91	27,18	15,1	33,24	15,22	26,78
Er:YAG laser	T0 (°C)		T1 (°C)		T2 (°C)	
	lowest	*highest*	*lowest*	*highest*	*lowest*	*highest*
1st cut	18,58	34,19	18,34	31,03	18,67	26,98
2nd cut	19,28	27,65	18,93	30,84	18,72	27,62

3rd cut	19,36	35,77	19,02	31,11	19,08	28,16
QMR scalpel	T0 (°C)		T1 (°C)		T2 (°C)	
	lowest	*highest*	*lowest*	*highest*	*lowest*	*highest*
1st cut	16,14	33,22	15,68	35,89*	16,01	26,18
2nd cut	17,42	26,32	17,7	39,01*	17,88	31,27
3rd cut	18,53	26,48	18,47	45,33*	17,76	28,78*
Nd:YAG laser	T0 (°C)		T1 (°C)		T2 (°C)	
	lowest	*highest*	*lowest*	*highest*	*lowest*	*highest*
1st cut	16,2	34,99	16,23	46,24*	16,35	24,71
2nd cut	16,24	41,67*	16,27	37,46*	15,94	26,26
3rd cut	16,32	35,19	16,23	35,67*	16,17	24,73
Er:YAG laser	T0 (°C)		T1 (°C)		T2 (°C)	
	lowest	*highest*	*lowest*	*highest*	*lowest*	*highest*
1st cut	18,03	33,01	17,55	33,13	18,74	27,77
2nd cut	18,19	34	18,25	34,2	19,14	28,04
3rd cut	18,74	28,69	18,72	30,97	18,95	28,11
QMR scalpel	T0 (°C)		T1 (°C)		T2 (°C)	
	lowest	*highest*	*lowest*	*highest*	*lowest*	*highest*
1st cut	13,94	34,7	14,64	33,74*	15,31	31,53
2nd cut	16,24	34,69	16,12	42,42*	15,71	31,01

3rd cut	14,79	34,25	14,85	44,67*	14,41	27,07
Nd:YAG laser	T0 (°C)		T1 (°C)		T2 (°C)	
	lowest	*highest*	*lowest*	*highest*	*lowest*	*highest*
1st cut	14,38	30,94	14,62	35,39*	14,7	28,89
2nd cut	14,13	24,37	14,98	42,1	14,81	27,5
3rd cut	18,21	35,24	18,38	38,51*	17,88	28

No variation of AF was highlighted for HT nor for both ST-A and ST-B within the thermal decay time.

DISCUSSION

Hard tissue (HT) samples:

Swine rib as hard tissue samples can be compared to human oral tissues due to its thickness and alveolar/cortical bone ratio.

Results showed that immediately after the incision the temperature's increase rapidly diminish and tissue samples resulted to be even at a lower temperature than the surrounding environment.

In one single case a high temperature value of 48,86 °C was detected within the sample tissue (Figure 31), it was localized in correspondence of the laser tip right after the cut was performed without water irrigation.

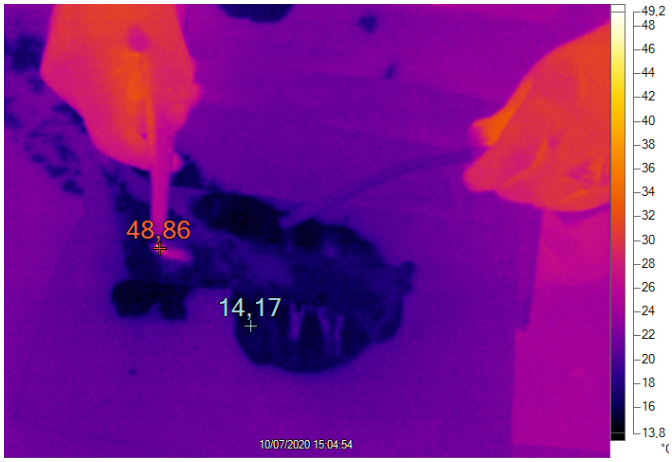

Figure 31: Detection of anomalus rise in temperature within hard tissue sample after Er:YAG incision without irrigation.

Explanation is to be identified in the lack of cleansing of the laser mirror: debris on the tip can capture the laser beam at the end of the hand piece resulting in an unwanted increase of temperature.

Laser users should frequently clean the mirror surface of the hand piece, more often if used without irrigation.

No main temperature variations were registered in presence or absence of irrigation.

This finding is particularly interesting: hemostasis can be increased by absence of water flow without any risk of damaging the surrounding tissues due to the temperature rise.

AF was not influenced by minimal temperature raises, either in presence or absence of water irrigation.

It was highlighted that AF was more intense by margins of the cut rather than the incision's floor (Figure 32), it can be hypothesize that expression of

endogenous fluorophores increases as interaction's time with laser light increases. Margins which represent the immediate periphery of the ablation area where the interaction with the laser beam lasts for a longer time (the total of the incision time) rather than the incision's floor which only interacts during the final phase of the cut.

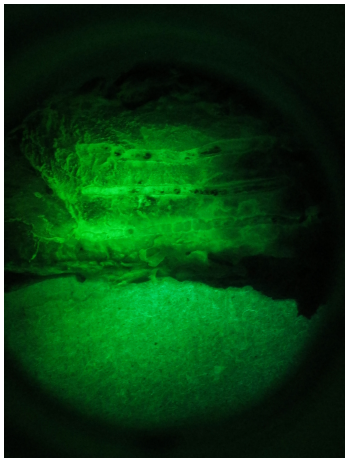

Figure 32: AF after Er:YAG incision on hard tissue sample: AF intensity is grater in margins rather than in the incision's floor.

However, no variation in the AF pattern has been observed during the thermal drop.

Soft tissue (ST-A, ST-B) samples:

Chicken soft tissue sample (ST-A) were selected as reference to less vascularized human oral tissue and liver soft tissue sample (ST-B) were selected as reference to more vascularized.

As highlighted in HT, Er:YAG laser even without irrigation involves a minimal thermal rise which falls within the incision time; its use for superficial ablation

can be combined to the hemostasis obtained by the minimal temperature increase.

Surgical instruments such as Nd:YAG laser and QRM are able to control bleeding during minor and major excision, allowing a better visibility in the surgical field and reducing the total surgical time but results of this study highlighted a significant temperature increase during incision and 30 seconds after.

Nd:YAG laser's wavelength has high selectivity for hemoglobin and poor water absorption and it allows to operate rapidly and with good hemostasis; the heat dissipation occurs rapidly and this tool can be used safely keeping in mind its ability to penetrate into the tissues up to about 7 mm.

The temperature increase is not to be ignored when these surgical instruments are used in order to benefit of their coagulating potential while respecting tissues around the surgical field.

As observed in HT, AF was not influenced by minimal nor greater temperature raises.

Even if AF was visibly more intense in ST rather than in HT, no main variation of AF pattern were highlighted within the thermal decay time.

This means that the fluorescence variations evidenced following the cut performed with lasers or QMR scalpel seem not to depend on the thermal variations caused by the instrument.

Also in ST-A (Figure 33) and ST-B (Figure 34) AF was more intense by margins of the cut rather than the incision's floor.

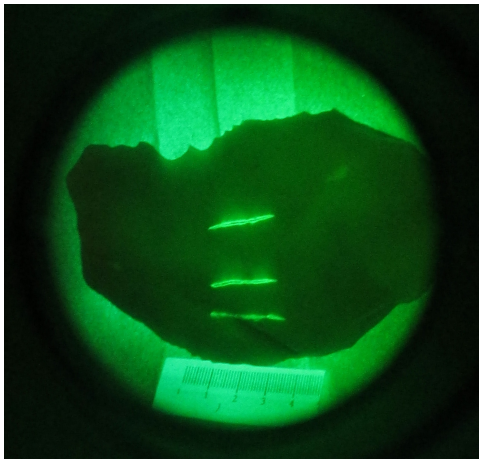

Figure 33: AF after Nd:YAG incision on soft chicken tissue sample: AF intensity is grater in margins rather than in the incision's floor.

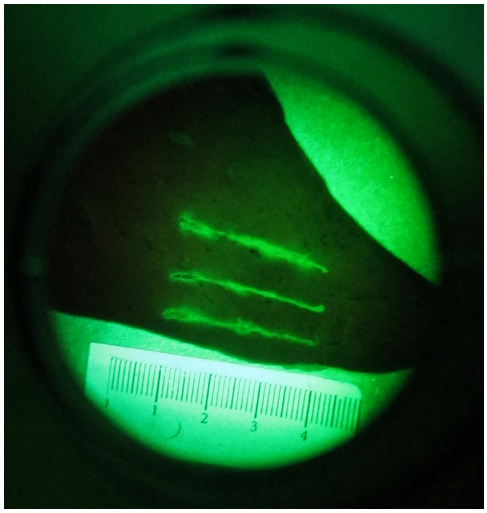

Figure 34: AF after RQM incision on soft liver tissue sample: AF intensity is grater in margins rather than in the incision's floor.

Moreover, the velscope system analyzes the fluorescence in a qualitatively way based on the image being displayed. A future goal will be to analyze the

fluorescence variations in a quantitative way, not only on the image but also on the tissue spectra.

More studies should be conducted to investigate these difference in endogenous fluochromes excitement.

This ex vivo study highlighted that incisions performed with Er:YAG laser, QMR scalpel and Nd:YAG laser lead to a detectable temperature rise that was completely dissipated within the 30 seconds following the cut.

The incision performed with Er:YAG laser, even without the cooling water system, did not show significant temperature rise in both hard and soft sample tissue, meaning that the coagulating effect obtained without irrigation can be used during superficial ablation without the risk of thermal damages.

Even if Nd:YAG laser cut showed the highest temperature peak during incision, in comparison to the QMR no significant differences in T1 nor T2 were highlighted.

This study also highlighted that auto-fluorescence was not influenced by temperature variations. AF was not altered by any of incisions performed with three of most common surgical instruments and most importantly no correlation between AF decay time and temperature decay time was found. Showing slow decay speed and stability over time, AF could be useful not only for screening before surgery but also for intra- and post-operative evaluations.

CONCLUSIONS

Tissue regeneration remains today a topic of great scientific interest on which researchers invest attention and resources with the aim of improving clinical strategies and therapeutic techniques.

Photobiomodulation has emerged as a completely non-invasive therapeutic option with large clinical positive implications.

Lasers with wavelength within the therapeutic window (ca. 600 nm to 1064 nm an further in the near and medium infrared spectrum) have been proven to be able to bost cell's internal bio-mechanism, resulting in a benefit of the irradiated tissues.

This work of thesis highlighted that laser application can lead to both cell's proliferation and differentiation improvement in all three investigated cell's line, although the implicated pathway's steps are yet to be completely understood.

It also emerged that between similar cell's line (of oncogenic nature) treated in our in vitro studies activations of intracellular mechanism were not identical and replicable, meaning that the precise target of PBM is yet to be identified.

PBM has been proven to be a safe treatment with no documentation of tissue damage, if applied by rigorous protocols of administration consisting in low doses per long periods of time.

This thesis work emphasized how no significant modification in tissue temperature are related to PBM, it is therefore a therapy applicable in all

subjects with the certainty of respecting all the neighbouring noble anatomical structures.

Aside, tis thesis work highlighted that disposable protections used to guarantee disinfection during medical laser treatments di not affect the delivery of laser light, a significant finding especially in a period of pandemic as was this one of COVID-19.

Even if PBM has widely been proven to lead to patient's clinical picture improvement, it remains a topic of study that will benefit from further insights, both with in vitro and in vivo studies.

Main focus for future studies may include the search for each steps and molecules involved in the cellular internalization of laser light in order to better target our therapies and the design of specific protocols for PBM for each section of application with particular attention to changes in values of autoflurescence.

Ringraziamenti

Ringrazio il professor Paolo Vescovi, mio tutor durante questi tre anni di dottorato ma principalmente mio mentore sin da prima della laurea.

Ringrazio profondamente il professor Roberto Sala, co-tutor di questa tesi, per la costante disponibilità, cortesia e dedizione al progetto e per tutto ciò che mi ha insegnato in questi anni.

Grazie al dottor Daniele Mori e a tutti i colleghi che mi hanno aiutata durante le numerose fasi di sperimentazione, mettendo a disposizione le loro conoscenze ed il loro tempo.

Grazie a tutto il gruppo di Patologia e Medicina Orale dell'Università di Parma, con i quali ho l'opportunità di collaborare quotidianamente e svolgere l'attività che più mi appassiona, ringrazio in particolare la professoressa Maddalena Manfredi.

In ultimo ma non per importanza, desidero ringraziare la mia famiglia ed i miei cari amici, per il loro sostegno e amore incondizionato che mi ha permesso di raggiungere questo ulteriore traguardo.

Bibliography

[1] K. T, "Is it time to consider photobiomodulation as a drug equivalent?," *Photomed Laser Surg.*, vol. May, no. 31(5), pp. 189–91, 2013.

[2] J. P. Tunér J, "Parameter Reproducibility in Photobiomodulation.," *Photomed Laser Surg.*, vol. Mar, no. 34(3), pp. 91–2, 2016.

[3] K. T. Passarella S, "Absorption of monochromatic and narrow band radiation in the visible and near IR by both mitochondrial and non-mitochondrial photoacceptors results in photobiomodulation.," *J Photochem Photobiol B.*, vol. Nov, no. 140, pp. 344–58, 2014.

[4] T. J., "The Laser Wound Healing Contradiction.," *Photomed Laser Surg.*, vol. Jun, no. 33(6), pp. 343–4, 2015.

[5] L. Abramovitch-Gottlib *et al.*, "Low level laser irradiation stimulates osteogenic phenotype of mesenchymal stem cells seeded on a three-dimensional biomatrix," *Lasers Med. Sci.*, vol. 20, no. 3–4, pp. 138–146, 2005, doi: 10.1007/s10103-005-0355-9.

[6] C. A. ugust. G. Barboza, F. Ginani, D. M. our. Soares, A. C. ristin. G. Henriques, and R. de A. Freitas, "Low-level laser irradiation induces in vitro proliferation of mesenchymal stem cells," *Einstein (Sao Paulo).*, vol. 12, no. 1, pp. 75–81, 2014, doi: 10.1590/S1679-45082014AO2824.

[7] S. Bouvet-Gerbettaz, E. Merigo, J. P. Rocca, G. F. Carle, and N. Rochet, "Effects of low-level laser therapy on proliferation and differentiation of murine bone marrow cells into osteoblasts and osteoelasts," *Lasers Surg. Med.*, vol. 41, no. 4, pp. 291–297, 2009, doi: 10.1002/lsm.20759.

[8] K. Choi *et al.*, "Low-level laser therapy promotes the osteogenic potential of adipose-derived mesenchymal stem cells seeded on an acellular dermal matrix," *J. Biomed. Mater. Res. - Part B Appl. Biomater.*, vol. 101 B, no. 6, pp. 919–928, 2013, doi: 10.1002/jbm.b.32897.

[9] F. D. P. Eduarde *et al.*, "Stem cell proliferation under low intensity laser irradiation: A preliminary study," *Lasers Surg. Med.*, vol. 40, no. 6, pp. 433–438, 2008, doi: 10.1002/lsm.20646.

[10] R. Fekrazad *et al.*, "The effects of combined low level laser therapy and mesenchymal stem cells on bone regeneration in rabbit calvarial defects," *J. Photochem. Photobiol. B Biol.*, vol. 151, no. 2015, pp. 180–185, 2015, doi: 10.1016/j.jphotobiol.2015.08.002.

[11] A. P. Fernandes *et al.*, "Effects of low-level laser therapy on stem cells from human exfoliated deciduous teeth," *J. Appl. Oral Sci.*, vol. 24, no. 4, pp. 332–337, 2016, doi: 10.1590/1678-775720150275.

[12] M. Giannelli *et al.*, "Photoactivation of bone marrow mesenchymal stromal cells with diode laser: Effects and mechanisms of action," *J. Cell. Physiol.*, vol. 228, no. 1, pp. 172–181, 2013, doi: 10.1002/jcp.24119.

[13] F. Hendudari, A. Piryaei, S. N. Hassani, H. Darbandi, and M. Bayat, “Combined effects of low-level laser therapy and human bone marrow mesenchymal stem cell conditioned medium on viability of human dermal fibroblasts cultured in a high-glucose medium,” *Lasers Med. Sci.*, vol. 31, no. 4, pp. 749–757, 2016, doi: 10.1007/s10103-016-1867-1.
[14] J. F. Hou, H. Zhang, X. Yuan, J. Li, Y. J. Wei, and S. S. Hu, “In vitro effects of low-level laser irradiation for bone marrow mesenchymal stem cells: Proliferation, growth factors secretion and myogenic differentiation,” *Lasers Surg. Med.*, vol. 40, no. 10, pp. 726–733, 2008, doi: 10.1002/lsm.20709.
[15] E. Merigo, S. Bouvet-Gerbettaz, F. Boukhechba, J. P. Rocca, C. Fornaini, and N. Rochet, “Green laser light irradiation enhances differentiation and matrix mineralization of osteogenic cells,” *J. Photochem. Photobiol. B Biol.*, vol. 155, pp. 130–136, 2016, doi: 10.1016/j.jphotobiol.2015.12.005.
[16] K. H. Min, J. H. Byun, C. Y. Heo, E. H. Kim, H. Y. Choi, and C. S. Pak, “Effect of Low-Level Laser Therapy on Human Adipose-Derived Stem Cells: In Vitro and In Vivo Studies,” *Aesthetic Plast. Surg.*, vol. 39, no. 5, pp. 778–782, 2015, doi: 10.1007/s00266-015-0524-6.
[17] C. Moura-Netto, L. S. Ferreira, C. M. Maranduba, A. C. V. Mello-Moura, and M. M. Marques, “Low-intensity laser phototherapy enhances the proliferation of dental pulp stem cells under nutritional deficiency,” *Braz. Oral Res.*, vol. 30, no. 1, pp. 1–6, 2016, doi: 10.1590/1807-3107BOR-2016.vol30.0080.
[18] B. Mvula, T. J. Moore, and H. Abrahamse, “Effect of low-level laser irradiation and epidermal growth factor on adult human adipose-derived stem cells,” *Lasers Med. Sci.*, vol. 25, no. 1, pp. 33–39, 2010, doi: 10.1007/s10103-008-0636-1.
[19] M. J. H. Nagata *et al.*, “Bone marrow aspirate combined with low-level laser therapy: A new therapeutic approach to enhance bone healing,” *J. Photochem. Photobiol. B Biol.*, vol. 121, pp. 6–14, 2013, doi: 10.1016/j.jphotobiol.2013.01.013.
[20] I. S. Park, P. S. Chung, and J. C. Ahn, “Adipose-derived stromal cell cluster with light therapy enhance angiogenesis and skin wound healing in mice,” *Biochem. Biophys. Res. Commun.*, vol. 462, no. 3, pp. 171–177, 2015, doi: 10.1016/j.bbrc.2015.04.059.
[21] L. O. Pereira, J. P. F. Longo, and R. B. Azevedo, “Laser irradiation did not increase the proliferation or the differentiation of stem cells from normal and inflamed dental pulp,” *Arch. Oral Biol.*, vol. 57, no. 8, pp. 1079–1085, 2012, doi: 10.1016/j.archoralbio.2012.02.012.
[22] T. S. de Oliveira *et al.*, “Effects of low level laser therapy on attachment, proliferation, and gene expression of VEGF and VEGF receptor 2 of adipocyte-derived mesenchymal stem cells cultivated under nutritional

deficiency," *Lasers Med. Sci.*, vol. 30, no. 1, pp. 217–223, 2015, doi: 10.1007/s10103-014-1646-9.
[23] D. M. Soares, F. Ginani, Á. G. Henriques, and C. A. G. Barboza, "Effects of laser therapy on the proliferation of human periodontal ligament stem cells," *Lasers Med. Sci.*, vol. 30, no. 3, pp. 1171–1174, 2015, doi: 10.1007/s10103-013-1436-9.
[24] M. Soleimani, E. Abbasnia, M. Fathi, H. Sahraei, Y. Fathi, and G. Kaka, "The effects of low-level laser irradiation on differentiation and proliferation of human bone marrow mesenchymal stem cells into neurons and osteoblasts-an in vitro study," *Lasers Med. Sci.*, vol. 27, no. 2, pp. 423–430, 2012, doi: 10.1007/s10103-011-0930-1.
[25] A. Theocharidou *et al.*, "Odontogenic differentiation and biomineralization potential of dental pulp stem cells inside Mg-based bioceramic scaffolds under low-level laser treatment," *Lasers Med. Sci.*, vol. 32, no. 1, pp. 201–210, 2017, doi: 10.1007/s10103-016-2102-9.
[26] H. Tuby, L. Maltz, and U. Oron, "Induction of autologous mesenchymal stem cells in the bone marrow by low-level laser therapy has profound beneficial effects on the infarcted rat heart," *Lasers Surg. Med.*, vol. 43, no. 5, pp. 401–409, 2011, doi: 10.1002/lsm.21063.
[27] J. Wang *et al.*, "MicroRNA-193 pro-proliferation effects for bone mesenchymal stem cells after low-level laser irradiation treatment through inhibitor of growth family, member 5," *Stem Cells Dev.*, vol. 21, no. 13, pp. 2508–2519, 2012, doi: 10.1089/scd.2011.0695.
[28] J. Y. Wu, C. H. Chen, C. Z. Wang, M. L. Ho, M. L. Yeh, and Y. H. Wang, "Low-Power Laser Irradiation Suppresses Inflammatory Response of Human Adipose-Derived Stem Cells by Modulating Intracellular Cyclic AMP Level and NF-κB Activity," *PLoS One*, vol. 8, no. 1, pp. 1–9, 2013, doi: 10.1371/journal.pone.0054067.
[29] I. M. Zaccara, F. Ginani, H. G. Mota-Filho, Á. C. G. Henriques, and C. A. G. Barboza, "Effect of low-level laser irradiation on proliferation and viability of human dental pulp stem cells," *Lasers Med. Sci.*, vol. 30, no. 9, pp. 2259–2264, 2015, doi: 10.1007/s10103-015-1803-9.
[30] P. Pandeshwar, M. D. Roa, R. Das, S. P. Shastry, R. Kaul, and M. B. Srinivasreddy, "Photobiomodulation in oral medicine: a review," *J. Investig. Clin. Dent.*, vol. 7, no. 2, pp. 114–126, 2016, doi: 10.1111/jicd.12148.
[31] D. Pastore, M. Greco, and S. Passarella, "Specific helium-neon laser sensitivity of the purified cytochrome c oxidase," *Int. J. Radiat. Biol.*, vol. 76, no. 6, pp. 863–870, 2000, doi: 10.1080/09553000050029020.
[32] T. I. Karu, "Mitochondrial signaling in mammalian cells activated by red and near-IR radiation," *Photochem. Photobiol.*, vol. 84, no. 5, pp. 1091–1099, 2008, doi: 10.1111/j.1751-1097.2008.00394.x.
[33] F. Zhang, L. Zhang, Y. Qi, and H. Xu, "Mitochondrial cAMP signaling," *Cell.*

Mol. Life Sci., vol. 73, no. 24, pp. 4577–4590, 2016, doi: 10.1007/s00018-016-2282-2.
[34] Z. Zhang, Q. Shen, X. Wu, D. Zhang, and D. Xing, "Activation of PKA/SIRT1 signaling pathway by photobiomodulation therapy reduces Aβ levels in Alzheimer's disease models," *Aging Cell*, vol. 19, no. 1, pp. 1–15, 2020, doi: 10.1111/acel.13054.
[35] M. R. Hamblin, Y. Y. Huang, S. K. Sharma, and J. Carroll, "Biphasic dose response in low level light therapy - an update," *Dose-Response*, vol. 9, no. 4, pp. 602–618, 2011, doi: 10.2203/dose-response.11-009.Hamblin.
[36] R. S. Ghidini G, Vescovi P, Meleti M, Giacomo S, Alessandro S, "Absorption capability of a 645-nm diode laser on swine soft tissue samples: a preliminary study in an ex- vivo model.," *J Dent Indones*, vol. 26, no. 75–80, 2019.
[37] F. Salehpour *et al.*, "Penetration Profiles of Visible and Near-Infrared Lasers and Light-Emitting Diode Light through the Head Tissues in Animal and Human Species: A Review of Literature," *Photobiomodulation, Photomedicine, Laser Surg.*, vol. 37, no. 10, pp. 581–595, 2019, doi: 10.1089/photob.2019.4676.
[38] S. L. Jacques, "Erratum: Optical properties of biological tissues: A review (Physics in Medicine and Biology (2013) 58)," *Phys. Med. Biol.*, vol. 58, no. 14, pp. 5007–5008, 2013, doi: 10.1088/0031-9155/58/14/5007.
[39] R. Alves and R. Grimalt, "A Review of Platelet-Rich Plasma: History, Biology, Mechanism of Action, and Classification," *Ski. Appendage Disord.*, vol. 4, no. 1, pp. 18–24, 2018, doi: 10.1159/000477353.
[40] P. R. Amable *et al.*, "Platelet-rich plasma preparation for regenerative medicine: Optimization and quantification of cytokines and growth factors," *Stem Cell Res. Ther.*, vol. 4, no. 3, pp. 1–13, 2013, doi: 10.1186/scrt218.
[41] E. Kobayashi *et al.*, "Comparative release of growth factors from PRP, PRF, and advanced-PRF," *Clin. Oral Investig.*, vol. 20, no. 9, pp. 2353–2360, 2016, doi: 10.1007/s00784-016-1719-1.
[42] M. Prideaux *et al.*, "SaOS2 osteosarcoma cells as an in vitro model for studying the transition of human osteoblasts to osteocytes," *Calcif. Tissue Int.*, vol. 95, no. 2, pp. 183–193, 2014, doi: 10.1007/s00223-014-9879-y.
[43] G. Ghiacci, S. Lumetti, E. Manfredi, D. Mori, G. M. Macaluso, and R. Sala, "Stanozolol promotes osteogenic gene expression and apposition of bone mineral in vitro," *J. Appl. Oral Sci.*, vol. 27, pp. 1–11, 2019, doi: 10.1590/1678-7757-2018-0014.
[44] et al. Martinotti S, Mazzucco L, Balbo V, "Platelet-rich plasma induces mixed osteogenic/osteoclastogenic pheno- type in osteosarcoma SaOS-2 cells: role of TGF-beta.," *Curr Pharm Biotechnol*, vol. 15, no. 120–126, 2014.
[45] Y. Ogino, Y. Ayukawa, T. Kukita, and K. Koyano, "The contribution of

platelet-derived growth factor, transforming growth factor-β1, and insulin-like growth factor-I in platelet-rich plasma to the proliferation of osteoblast-like cells," *Oral Surgery, Oral Med. Oral Pathol. Oral Radiol. Endodontology*, vol. 101, no. 6, pp. 724–729, 2006, doi: 10.1016/j.tripleo.2005.08.016.

[46] A. M. Deana, A. M. de Souza, V. P. Teixeira, R. A. Mesquita-Ferrari, S. K. Bussadori, and K. P. S. Fernandes, "The impact of photobiomodulation on osteoblast-like cell: a review," *Lasers Med. Sci.*, vol. 33, no. 5, pp. 1147–1158, 2018, doi: 10.1007/s10103-018-2486-9.

[47] B. Chang *et al.*, "The effects of photobiomodulation on MC3T3-E1 cells via 630 nm and 810 nm light-emitting diode," *Med. Sci. Monit.*, vol. 25, pp. 8744–8752, 2019, doi: 10.12659/MSM.920396.

[48] V. Aleksic *et al.*, "Low-level Er: YAG laser irradiation enhances osteoblast proliferation through activation of MAPK/ERK," *Lasers Med. Sci.*, vol. 25, no. 4, pp. 559–569, 2010, doi: 10.1007/s10103-010-0761-5.

[49] A. Tani, F. Chellini, M. Giannelli, D. Nosi, S. Zecchi-Orlandini, and C. Sassoli, "Red (635 nm), near-infrared (808 nm) and violet-blue (405 nm) photobiomodulation potentiality on human osteoblasts and mesenchymal stromal cells: A morphological and molecular in vitro study," *Int. J. Mol. Sci.*, vol. 19, no. 7, pp. 1–23, 2018, doi: 10.3390/ijms19071946.

[50] C. Chavez Kappel, M. C. Velez-Yanguas, S. Hirschfeld, and L. J. Helman, "Human Osteosarcoma Cell Lines Are Dependent on Insulin-like Growth Factor I for in Vitro Growth," *Cancer Res.*, vol. 54, no. 10, pp. 2803–2807, 1994.

[51] T. D. Moreiras H, O'Connor C, Bell M, "Visible light and human skin pigmentation: The importance of skin phototype.," *Exp Dermatol.*, vol. 30, no. 9, pp. 1324-1331., 2021.

[52] W. A. of L. T. (WALT)., "Consensus agreement on the design and conduct of clinical studies with low-level laser therapy and light therapy for musculoskeletal pain and and conduct of clinical studies with low-level laser therapy and light therapy for musculoskeletal pain and disor," *Photomed Laser Surg.*, vol. 24, no. 6, pp. 761–2., 2006.

[53] et al. Makihara E, Makihara M, Masumi S, "Evaluation of facial thermographic changes before and after low-level laser irradiation.," *Photomed Laser Surg.*, vol. 23, no. 2, pp. 191–5.

[54] et al. Stadler I, Lanzafame RJ, Oskoui P, "Alteration of skin temperature during low-level laser irradiation at 830 nm in a mouse model.," *Photomed Laser Surg.*, vol. 22, no. 3, pp. 227–31.

[55] et al. Grandinétti Vdos S, Miranda EF, Johnson DS, "The thermal impact of phototherapy with concurrent super-pulsed lasers and red and infrared LEDs on human skin.," *Lasers Med Sci.*, vol. 30, no. 5, pp. 1575–81.

[56] et al. Souza-Barros L, Dhaidan G, Maunula M, "Skin color and tissue

thickness effects on transmittance, reflectance, and skin temperature when using 635 and 808 nm lasers in low intensity therapeutics.," *Lasers Surg Med.*, vol. 50, no. 4, pp. 291-301.
[57] et al. Joensen J, Demmink JH, Johnson MI, "The thermal effects of therapeutic lasers with 810 and 904 nm wavelengths on human skin.," *Photomed Laser Surg.*, vol. 29, no. 3, pp. 145–53., 2011.
[58] V. S. G. M. Agarwal M, "Efficacy of a Low Fluence, High Repetition Rate 810nm Diode Laser for Permanent Hair Reduction in Indian Patients with Skin Types IV-VI.," *J Clin Aesthet Dermatol.*, vol. 9, no. 11, pp. 29-33.
[59] P. V. Sadick NS, "The use of a new diode laser for hair removal.," *Dermatol Surg.*, vol. 29, no. 1, pp. 30–3.
[60] G. C. Taub AF, "Treatment of Acne Scars of Skin Types II to V by Sublative Fractional Bipolar Radiofrequency and Bipolar Radiofrequency Combined with Diode Laser.," *J Clin Aesthet Dermatol.*, vol. Oct;, no. 4, pp. 18–27, 2011.
[61] et al. Jih MH, Friedman PM, Goldberg LH, "The 1450-nm diode laser for facial inflammatory acne vulgaris: dose-response and 12-month follow-up study.," *J Am Acad Dermatol.*, vol. Jul, no. 55, pp. 80–7, 2006.
[62] et al. Chua SH, Ang P, Khoo LS, "Nonablative 1450-nm diode laser in the treatment of facial atrophic acne scars in type IV to V Asian skin: a prospective clinical study.," *Dermatol Surg.*, vol. 30, no. 10, pp. 1287–91, 2004.
[63] A. Mehl, L. Kremers, K. Salzmann, and R. Hickel, "3D volume-ablation rate and thermal side effects with the Er:YAG and Nd:YAG laser.," *Dent. Mater.*, vol. 13, no. 4, pp. 246–251, 1997, doi: 10.1016/S0109-5641(97)80036-X.
[64] W. L. Al-Batayneh OB, Seow WK, "Assessment of Er:YAG laser for cavity preparation in primary and permanent teeth: a scanning electron microscopy and thermographic study.," *Pediatr Dent.*, vol. 36(3), no. 90–94, 2014.
[65] L. Tiwari, O. Kujan, and C. S. Farah, "Optical fluorescence imaging in oral cancer and potentially malignant disorders: A systematic review," *Oral Dis.*, vol. 26, no. 3, pp. 491–510, 2020, doi: 10.1111/odi.13071.
[66] I. Pavlova, M. Williams, A. El-Naggar, R. Richards-Kortum, and A. Gillenwater, "Understanding the biological basis of autofluorescence imaging for oral cancer detection: High-resolution fluorescence microscopy in viable tissue," *Clin. Cancer Res.*, vol. 14, no. 8, pp. 2396–2404, 2008, doi: 10.1158/1078-0432.CCR-07-1609.
[67] N. Bhatia, M. A. T. Matias, and C. S. Farah, "Assessment of a decision making protocol to improve the efficacy of VELscope™ in general dental practice: A prospective evaluation," *Oral Oncol.*, vol. 50, no. 10, pp. 1012–1019, 2014, doi: 10.1016/j.oraloncology.2014.07.002.
[68] H. Hanken *et al.*, "Correction to The detection of oral pre- malignant lesions with an autofluorescence based imaging system (VELscopeTM) - a single

blinded clinical evaluation [Head Face Med, 9 (2013) 21]," *Head Face Med.*, vol. 9, no. 1, pp. 1–7, 2013, doi: 10.1186/1746-160X-9-26.
[69] I. Giovannacci, P. Vescovi, M. Manfredi, and M. Meleti, "Non-invasive visual tools for diagnosis of oral cancer and dysplasia: A systematic review," *Med. Oral Patol. Oral y Cir. Bucal*, vol. 21, no. 3, pp. e305–e315, 2016, doi: 10.4317/medoral.20996.
[70] I. Giovannacci *et al.*, "Erratum to: Advantages of new technologies in oral mucosal surgery: an intraoperative comparison among Nd:YAG laser, quantic molecular resonance scalpel, and cold blade [Lasers in Medical Science, 10.1007/s10103-015-1769-7]," *Lasers Med. Sci.*, vol. 30, no. 7, p. 1911, 2015, doi: 10.1007/s10103-015-1793-7.
[71] P. Vescovi *et al.*, "Quantic molecular resonance scalpel and its potential applications in oral surgery," *Br. J. Oral Maxillofac. Surg.*, vol. 46, no. 5, pp. 355–357, 2008, doi: 10.1016/j.bjoms.2007.09.014.
[72] Coluzzi DJ., "Lasers in dentistry.," *Lasers Dent. Compend Contin Educ Dent.*, vol. Jun, no. 26(6A Suppl), pp. 429–35; quiz 436., 2005.
[73] K. I. Bader C, "Indications and limitations of Er:YAG laser applications in dentistry.," *Am J Dent.*, vol. Jun, no. 19(3), pp. 178–86, 2006.
[74] D. Yi, X. Shimeng, and Y. Heng, "Nd : YAG 激光在口腔医学中的□用," 2015.
[75] P. Vescovi, E. Merigo, C. Fornaini, J. P. Rocca, and S. Nammour, "Thermal increase in the oral mucosa and in the jawbone during Nd: YAG laser applications. Ex vivo study," *Med. Oral Patol. Oral Cir. Bucal*, vol. 17, no. 4, pp. 0–7, 2012, doi: 10.4317/medoral.17726.
[76] Y. Kimura, D.-G. Yu, A. Fujita, A. Yamashita, Y. Murakami, and K. Matsumoto, "Effects of Erbium, Chromium:YSGG Laser Irradiation on Canine Mandibular Bone," *J. Periodontol.*, vol. 72, no. 9, pp. 1178–1182, 2001, doi: 10.1902/jop.2000.72.9.1178.
[77] W. Van Den Bos *et al.*, "Thermal Energy during Irreversible Electroporation and the Influence of Different Ablation Parameters," *J. Vasc. Interv. Radiol.*, vol. 27, no. 3, pp. 433–443, 2016, doi: 10.1016/j.jvir.2015.10.020.
[78] I. Giovannacci, M. Meleti, D. Corradi, and P. Vescovi, "Clinical Differences in Autofluorescence Between Viable and Nonvital Bone: A Case Report With Histopathologic Evaluation Performed on Medication-Related Osteonecrosis of the Jaws," *J. Oral Maxillofac. Surg.*, vol. 75, no. 6, pp. 1216–1222, 2017, doi: 10.1016/j.joms.2016.12.011.
[79] T. P. Do, G. F. Heldarskard, L. T. Kolding, J. Hvedstrup, and H. W. Schytz, "Myofascial trigger points in migraine and tension-type headache," *J. Headache Pain*, vol. 19, no. 1, p. 84, 2018, doi: 10.1186/s10194-018-0913-8.
[80] A. Shimatani, M. Hoshi, N. Oebisu, T. Iwai, N. Takada, and H. Nakamura, "Clinical significance of thermal detection of soft-tissue tumors," *Int. J. Clin. Oncol.*, vol. 25, no. 7, pp. 1418–1424, 2020, doi: 10.1007/s10147-020-

01658-1.
[81] E. Sanchis-Sánchez, C. Vergara-Hernández, R. M. Cibrián, R. Salvador, E. Sanchis, and P. Codoñer-Franch, “Infrared thermal imaging in the diagnosis of musculoskeletal injuries: A systematic review and meta-analysis,” *Am. J. Roentgenol.*, vol. 203, no. 4, pp. 875–882, 2014, doi: 10.2214/AJR.13.11716.